Earth Syst. Sci. Data, 9, 221–249, 2017
www.earth-syst-sci-data.net/9/221/2017/
doi:10.5194/essd-9-221-2017

Open Access Earth System Science Data

A high space–time resolution dataset linking meteorological forcing and hydro-sedimentary response in a mesoscale Mediterranean catchment (Auzon) of the Ardèche region, France

Guillaume Nord[1], Brice Boudevillain[1], Alexis Berne[2], Flora Branger[3], Isabelle Braud[3], Guillaume Dramais[3], Simon Gérard[1], Jérôme Le Coz[3], Cédric Legoût[1], Gilles Molinié[1], Joel Van Baelen[4], Jean-Pierre Vandervaere[1], Julien Andrieu[5], Coralie Aubert[1], Martin Calianno[1,6], Guy Delrieu[1], Jacopo Grazioli[2], Sahar Hachani[1,7], Ivan Horner[3], Jessica Huza[3,8,a], Raphaël Le Boursicaud[3], Timothy H. Raupach[2], Adriaan J. Teuling[8], Magdalena Uber[1,9], Béatrice Vincendon[10], and Annette Wijbrans[1]

[1]Univ. Grenoble Alpes, CNRS, IRD, Grenoble INP, IGE, 38000 Grenoble, France
[2]Environmental Remote Sensing Laboratory (LTE), École Polytechnique Fédérale de Lausanne (EPFL), Lausanne, Switzerland
[3]Irstea, UR HHLY, Hydrology-Hydraulics, Villeurbanne, France
[4]LaMP, CNRS/UBP, Clermont Ferrand, France
[5]Université Côte d'Azur, CNRS, ESPACE, France
[6]Institut de géographie et durabilité, Université de Lausanne, Lausanne, Switzerland
[7]École Nationale d'Ingénieurs de Tunis, Université de Tunis, El Manar 1, Tunisia
[8]Hydrology and Quantitative Water Management Group, Wageningen University & Research, Wageningen, the Netherlands
[9]Institute of Earth and Environmental Science, University of Potsdam, Potsdam, Germany
[10]CNRM UMR 3589 (Météo-France & CNRS), Toulouse, France
[a]now at: Amec Foster Wheeler Environment and Infrastructure, 1425 Route Transcanadienne, Dorval, H9P 2W9, Québec, Canada

Correspondence to: Guillaume Nord (guillaume.nord@univ-grenoble-alpes.fr)

Received: 19 July 2016 – Discussion started: 23 September 2016
Revised: 16 December 2016 – Accepted: 22 January 2017 – Published: 22 March 2017

Abstract. A comprehensive hydrometeorological dataset is presented spanning the period 1 January 2011–31 December 2014 to improve the understanding of the hydrological processes leading to flash floods and the relation between rainfall, runoff, erosion and sediment transport in a mesoscale catchment (Auzon, 116 km^2) of the Mediterranean region. Badlands are present in the Auzon catchment and well connected to high-gradient channels of bedrock rivers which promotes the transfer of suspended solids downstream. The number of observed variables, the various sensors involved (both in situ and remote) and the space–time resolution ($\sim km^2$, $\sim$ min) of this comprehensive dataset make it a unique contribution to research communities focused on hydrometeorology, surface hydrology and erosion. Given that rainfall is highly variable in space and time in this region, the observation system enables assessment of the hydrological response to rainfall fields. Indeed, (i) rainfall data are provided by rain gauges (both a research network of 21 rain gauges with a 5 min time step and an operational network of 10 rain gauges with a 5 min or 1 h time step), S-band Doppler dual-polarization radars (1 km^2, 5 min resolution), disdrometers (16 sensors working at 30 s or 1 min time step) and Micro Rain Radars (5 sensors, 100 m height resolution). Additionally, during the special observation period (SOP-1) of the HyMeX (Hydrological Cycle in the Mediterranean Experiment) project, two X-band radars provided precipitation measurements at

very fine spatial and temporal scales (1 ha, 5 min). (ii) Other meteorological data are taken from the operational surface weather observation stations of Météo-France (including 2 m air temperature, atmospheric pressure, 2 m relative humidity, 10 m wind speed and direction, global radiation) at the hourly time resolution (six stations in the region of interest). (iii) The monitoring of surface hydrology and suspended sediment is multi-scale and based on nested catchments. Three hydrometric stations estimate water discharge at a 2–10 min time resolution. Two of these stations also measure additional physico-chemical variables (turbidity, temperature, conductivity) and water samples are collected automatically during floods, allowing further geochemical characterization of water and suspended solids. Two experimental plots monitor overland flow and erosion at 1 min time resolution on a hillslope with vineyard. A network of 11 sensors installed in the intermittent hydrographic network continuously measures water level and water temperature in headwater subcatchments (from 0.17 to 116 km^2) at a time resolution of 2–5 min. A network of soil moisture sensors enables the continuous measurement of soil volumetric water content at 20 min time resolution at 9 sites. Additionally, concomitant observations (soil moisture measurements and stream gauging) were performed during floods between 2012 and 2014. Finally, this dataset is considered appropriate for understanding the rainfall variability in time and space at fine scales, improving areal rainfall estimations and progressing in distributed hydrological and erosion modelling.

DOI of the referenced dataset: doi:10.6096/MISTRALS-HyMeX.1438.

1 Introduction

The Mediterranean area is prone to intense rainfall events, sometimes triggering flash floods that may have dramatic consequences (Ruin et al., 2008). Flash floods are the consequence of short, high-intensity rainfalls mainly of spatially confined convective origin and often enhanced by orography (Borga et al., 2014). Therefore, flash floods usually impact basins less than 1000 km^2 (Marchi et al., 2010). In medium-scale Mediterranean catchments, the control exerted by the amount of rainfall and its intensity and variability on the generation of runoff and the erosional processes operating at different scales is of major importance (Navratil et al., 2012; Marra et al., 2014; Tuset et al., 2016). Assisting stakeholders in implementing efficient soil conservation and river management measures implies understanding the processes and the factors that control surface runoff, developing modelling approaches able to provide reliable flow separations, localizing sediment sources and sinks, and predicting the space–time dynamics of sediment and associated contaminant within the catchment. This requires taking into account the space–time variability in rainfall events, using spatially distributed models coupling hydrology and mass transfers.

Although the interest for distributed models is recognized for understanding the inner behaviour of the catchment (i.e. pathways and transit times), many studies have shown that their reliability does not meet the expectations. Indeed, the water and sediment discharges simulated by distributed models at the outlet of the catchment are generally poorer than the results simulated by lumped models (Jetten et al., 2003; Reed et al., 2004; de Vente el al., 2013). To date there are various difficulties that hinder the potential of distributed models (e.g. Cea et al., 2016) such as the large number of parameters, the definition of some parameters which are difficult to measure, the high non-linearity of the equations, the interaction between input parameters, the uncertainty in the experimental measurements and input data, the space–time variability in the physical processes, and the lack of comprehensive field data available for initialization and calibration. Thus, the deployment of multi-scale observation systems over a period of several years in medium catchments and the release of the collected datasets as open data with metadata on how the data have been collected and quality-assured, as well as their associated uncertainties (Weiler and Beven, 2015), are of crucial importance to address the current limitations of distributed models.

High space–time resolution ($\sim km^2$, $\sim$ min) datasets linking meteorological forcing and hydro-sedimentary response are rare in scientific literature because of the high number and diversity of types of sensors required for measuring rainfall and surface hydrology. The already published datasets consist of first-order catchments ("Tarrawarra data set", southeastern Australia: Western and Grayson, 1998), catchments where the observation period is exceptionally long ("Reynolds Creek Experimental Watershed", northwestern USA: Slaughter et al., 2001; "Walnut Gulch Experimental Watershed", southwestern USA: Renard et al., 2008; Stone et al., 2008; "Goodwater Creek Experimental Watershed and Salt River Basin", midwestern USA: Baffaut et al., 2013), or catchments located in snow-dominated mountains ("Reynolds Creek Experimental Watershed", northwestern USA: Reba et al., 2011; "Dry Creek Experimental Watershed", northwestern USA: Kormos et al., 2014). In mesoscale catchments, such datasets are scarce ("Walnut Gulch Experimental Watershed", southwestern USA: Goodrich et al., 1997; "Iowa River Basin", north central USA: Gupta et al., 2010), especially in the Mediterranean region.

This study is part of the FloodScale project (Braud et al., 2014), which is a contribution to the HyMeX programme (Hydrological Cycle in the Mediterranean Experiment, Drobinski et al., 2014), a 10-year multidisciplinary programme on the Mediterranean water cycle. A three-level nested experimental strategy was planned for the HyMeX programme:

- A long-term observation period (LOP) lasting about 10 years (2010–2020) to gather and provide observations of the whole coupled system that support analysis of the seasonal-to-interannual variability in the water cycle through budget analyses.
- An enhanced observation period (EOP) lasting about 5 years (2011–2015), for both budget and process studies.
- Special observation periods (SOPs) of several months, which aimed at providing detailed and specific observations to study key processes of the water cycle in specific Mediterranean regions, with emphases put on heavy precipitation systems and intense air–sea fluxes and dense water formation.

The FloodScale project (2012–2015) fits into the EOP and encompasses SOP1 (Ducrocq et al., 2014), which took place from 5 September to 6 November 2012 and was dedicated to heavy precipitation and flash floods. This study focuses on nested scales that range from the hillslope to the medium catchment scale, all belonging to the Cévennes – Vivarais Mediterranean Hydrometeorological Observatory (OHMCV) (Boudevillain et al., 2011). It is located in Ardèche, in a region with a high gradient in annual rainfall (e.g. Molinié et al., 2012). The observation system was operated by different teams from various countries during SOP1 and the EOP: IGE, IRSTEA Lyon, EPFL, Wageningen University, LaMP and Météo-France. The dataset includes precipitation and weather data, soil moisture data, runoff and soil erosion data, hydrologic and suspended sediment response data, surface water quality data, and GIS data.

The duration of the observations presented here (4 years, from 1 January 2011 to 31 December 2014) allows the characterization of the standard catchment behaviour and provides the opportunity to observe less ordinary events with processes that are specific to flash floods and to characterize possible threshold effects that are not observed in small to moderate events. The observation strategy is reinforced by the deployment of conventional and polarimetric radars that provide precipitation measurements at spatial scales not properly resolved by rain gauge networks (Berne and Krajewski, 2013). A special effort was dedicated to soil moisture measurements and stream gauging during floods. These opportunistic observations made possible by a real-time warning system enable watching transient processes like runoff, monitoring the increase in water content in soil and gauging high discharges in small to medium catchments, which is challenging due to the very short response times of such systems. This allows documenting the upper ends of stage–discharge rating curves that are generally extrapolated at high values.

The paper presents the acquired datasets to make them accessible to the scientific community and make their use easier and wider. The authors are convinced that the published datasets can serve as a benchmark for hydrological distributed modelling applied to the Mediterranean area. The paper is organized as follows. Section 2 presents the location of the studied catchment and its context (geology, climatology, land use, pedology). Section 3 describes the observation system (instruments and measured variables) and is organized into three subsections: (i) hydrometeorological data, (ii) spatial characterization data, and (iii) hydrological and sediment data. Finally, in Sect. 4, the first studies that provide preliminary answers to the scientific questions selected in the introduction are highlighted.

2 Catchment description

The Auzon catchment (116 km^2) is located in a region traditionally called "Bas Vivarais" between the plains of the Rhône Valley to the east (minimum elevation: 40 m a.s.l.) and the Ardèche Mountains to the west (maximum elevation: 1550 m a.s.l.). The Auzon River is a left-bank tributary of the Ardèche River, which drains from north to south (Fig. 1). The Auzon catchment ranges in elevation from 140 to 1019 m a.s.l. This mid-elevation area includes the volcanic plateau of Coiron to the north (approximately one-third of the catchment area), standing as a barrier. The latter closes the horizon over the sedimentary piedmont hills to the south (approximately two-thirds of the catchment area). The Coiron Plateau is a vast basaltic table ranging in elevation from 600 to 1000 m that has the appearance of an oak leaf lying on the marly-limestone bedrock of the Bas Vivarais (Grillot, 1971; Naud, 1972). Intense volcanic activity between 7.7 and 6.4 million years BP (early Pliocene) produced stacked lava flows and pyroclastic flows that gradually filled a former valley. This phase of volcanic activity is contemporaneous with the volcanism phase of the Mont Mézenc. The current morphology of the region is the result of significant Quaternary erosion, which has notched the edges of the lava flows delimiting narrow digitations separated by marly thalwegs. An inverted relief is now observed where the present surface of the plateau corresponds to the former valley bottom. The sedimentary substratum is composed of Cretaceous marls and limestones from the Upper Jurassic. The former valley bottom is now raised with respect to the young valleys carved by streams and one can observe gorges with steep slopes of marls with a typical badlands aspect.

The region is exposed to both oceanic and Mediterranean climatic influences. The terrain of the region is partly mountainous and plays a major role on rainfall properties. The

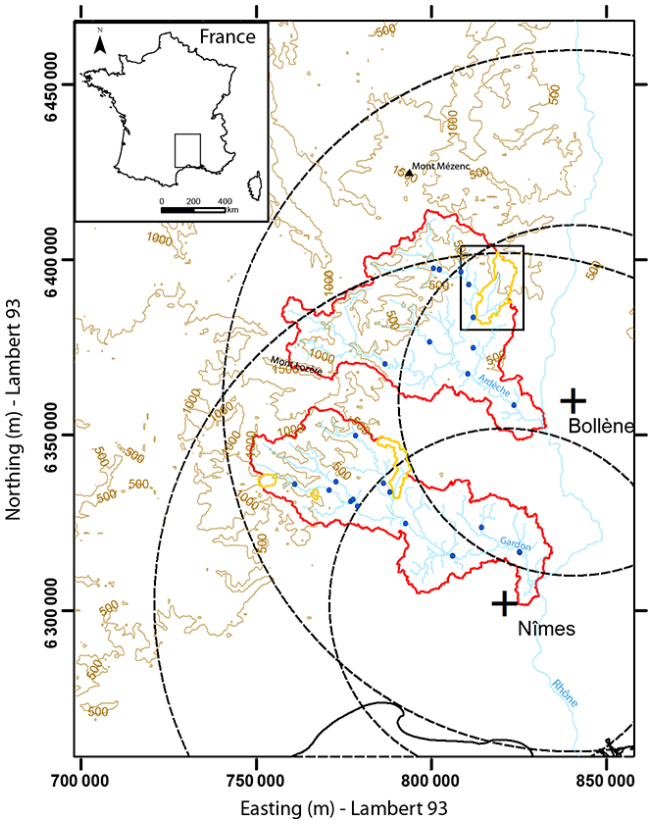

Figure 1. Location of the OHMCV pilot site. The two main catchments studied in the FloodScale project (Braud et al., 2014) – Gardon (2062 km^2) in the south and Ardèche (2388 km^2) in the north – are outlined by the bold red line along with the main rivers and the operational hydrometric stations (blue dots). The small research catchments are shown with orange boundaries. The Auzon catchment, which is the object of this study, is framed by a black rectangle which defines the spatial extension of Fig. 3. The two S-band operational radars with the range circles at 50 and 100 km (dashed circles) are also shown. The 500 m contour lines are displayed in the background.

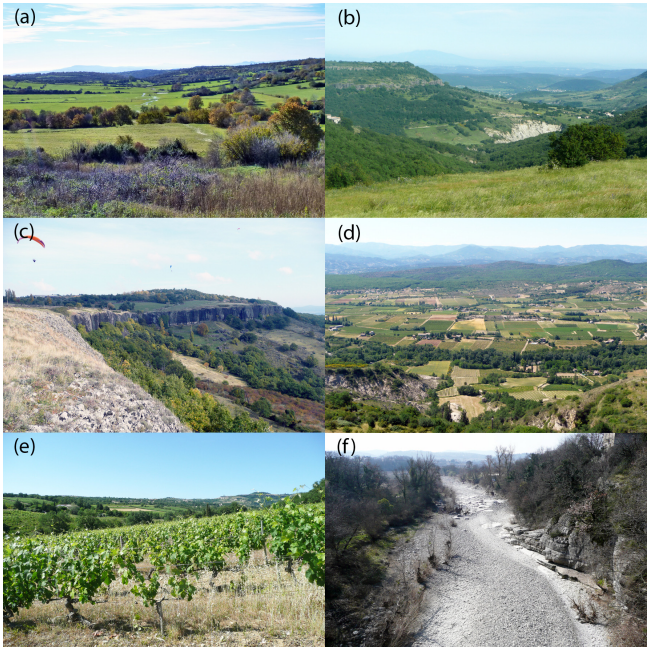

Figure 2. Typical landscapes of the Auzon catchment: **(a)** volcanic plateau of Coiron with a mix of grassland and open woodlands in the north part of the catchment, **(b)** deep valleys descending from the Coiron Plateau presenting steep slopes of marls with badlands aspects and covered by deciduous forest, **(c)** southern boundary of the Coiron Plateau characterized by the presence of cliffs, **(d)** toposequence on marly-limestone formations with regosols on steep marly slopes in the foreground followed by cultivated clayey soils with vines and ending with rocky outcrops and lithosols on limestones with garrigue, **(e)** hillslopes with vineyards on clayey soils drained by a river incised in the marly-limestone bedrock and surrounded by a zone of riparian vegetation, and **(f)** garrigue and Mediterranean open woodland on karstified limestones in the western part of the catchment leading to the rapid drying-up of the Auzon River.

highest average daily rainfall intensities are located in the higher areas, while the highest average hourly rainfall intensities are located over the plain (Molinié et al., 2012). Average yearly rainfall ranges between 850 and 900 mm throughout the Auzon Basin, which represents an intermediate value between the plains of the Rhône Valley to the east (500 mm) and the Ardèche Mountains to the west (2000 mm).

On the Coiron Plateau, forest vegetation has almost completely disappeared (Figs. 2 and 3b). Oaks, chestnut trees and associated shrub flora only remain on the marly slopes and basalt screes. Mediterranean grazed open woodlands with broom (*Sarothamnus purgans*), boxwood (*Buxus sempervirens*) and sloe tree (*Prunus spinosa*) cover almost all the rocky outcrops (Bornand et al., 1977). Grasslands and crops are located in well-drained depressions.

On most of the limestone formations and marly formations with steep slopes, natural vegetation is dominant. This vegetation consists of downy oak woods (*Quercus pubescens*), garrigues and Mediterranean open woodlands where stunted oaks are associated with broom (*Sarothamnus purgans*), boxwood (*Buxus sempervirens*), juniper and dry grasslands (thyme, *Aphyllanthes* and *Brachypodium*). On marly-limestone formations with low slope, the vegetation has been cleared and gave way to traditional crops (cereals, vines, etc.) and grazed grassland. Overall, according to the CORINE Land Cover 2006 classification, the Auzon catchment consists of forest (26.7 %); pastures under agricultural use (17.1 %); vineyards (19 %); moors, heathland and sparsely vegetated areas (14.3 %), crops (9.5 %); natural grasslands (11 %); and urban areas (2.3 %).

The brown soils on basalt material cover the majority of the volcanic edifice of the Coiron Plateau (Fig. 3c). They gather soils supported by basaltic rock (16a), scoria and tuffs

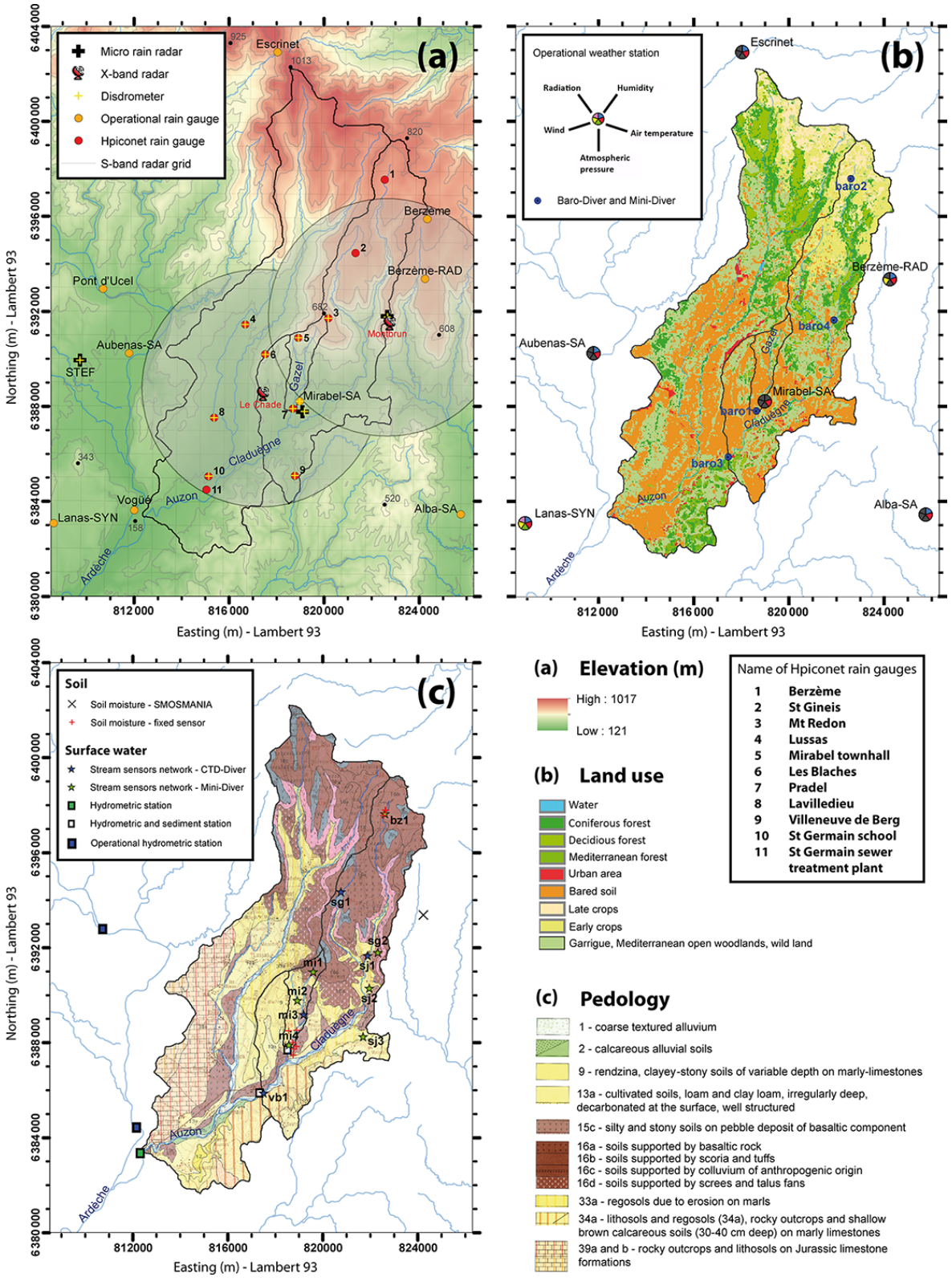

Figure 3. Location maps of the Auzon catchment and instruments for **(a)** rainfall, **(b)** meteorology, and **(c)** hydrology. Three different backgrounds are represented: **(a)** elevation (25 m bare-earth DEM, source: IGN), **(b)** land use (30 m resolution images derived from Landsat images, source: UMR Espace), and **(c)** (1 : 100 000 soil map, source: INRA). Icons for X-band radars from the IFLOODS project website (http://ifis.iowafloodcenter.org/ifis/more/ifloods/) (Demir et al., 2015).

(16b), colluvium of anthropogenic origin (16c), screes and talus fans (16d). These four main soil families constitute a very homogeneous group with very close physico-chemical characteristics. Cartographic differences are based on the nature of the parent rock, the topographic location and human intervention; those factors determine the depth, the heterogeneity and the texture of soils (Bornand et al., 1977). Soil depths are generally less than 2 m. The soil matrix consists mainly of clay and fine silt. The stony load is variable according to the drainage of the medium.

In the piedmont hills beneath the Coiron Plateau, there are rendzina (9), clayey-stony soils of variable depth (20–70 cm) on marly limestones and regosols (33a) due to erosion on marls characterized by deep gullies (badlands) that constitute a significant source of suspended material during floods. In less steep terrain, there are generally cultivated soils (13a), loam and clay loam that are irregularly deep, decarbonated at the surface, well structured and supporting cereal crops and vines. At the south of the Auzon catchment, there are lithosols and regosols (34a), rocky outcrops and shallow brown calcareous soils (30–40 cm deep) on marly limestones. On the western edge of the Auzon catchment, rocky outcrops and lithosols (39a and b) on Jurassic limestone formations are highly dominant. These karstified formations are responsible for the natural drying-up of the Auzon River, frequently observed in its downstream reach. Finally, on the edges of the main rivers (Claduègne and Auzon), calcareous alluvial soils (2) or coarse textured alluvium (1) are present.

The multi-scale observation system presented in this study (Fig. 3) is based on nested catchments: the Gazel catchment (3.4 km^2), the Claduègne catchment (44 km^2) and the Auzon catchment (116 km^2). Rainfall and weather observations include both operational and research instruments that are located both inside the catchments and in their immediate vicinity. Hydrological observations are mainly concentrated over the Claduègne catchment.

3 Data description

Table 1 presents the hydrometeorological variables, gives the characteristics and the number of instruments, and indicates whether the measurements belong to an operational network or a research network of observation. Table 2 presents the soil and surface water variables (hydrological and sediment data) and gives the characteristics and the number of instruments. Table A2 in Appendix A contains a chart that describes the period of measurement of each instrument (rainfall, meteorology, soil and surface water) and specifies the number of instruments deployed in the field. All the data presented here have undergone careful (mostly manual) quality assurance.

3.1 Hydrometeorological data

3.1.1 Rainfall

Radars

The region of interest is covered by two operational S-band radars (Fig. 1): a conventional radar (Thomson MTO 2000S) located in Bollène (about 40 km away) and a polarimetric radar (Selex Meteor 600S) located in Nîmes (about 90 km away). Their visibility over the Auzon catchment is, however, hindered by the topography and the lowest beam is at about 2 km above the ground. These operational radars, managed by Météo-France, provided data (radar reflectivity and rain rate estimates) over the entire period of interest. To complement these radars and monitor the small-scale variability in precipitation, two additional X-band research radars were deployed during HyMeX SOP1 (Fig. 3a), providing measurements at a resolution of about 100 m × 100 m. A fast-scanning radar (WR-10X+), managed by LaMP, provided rapid plan position indicator (PPI) scans (every 3 min) at one elevation. EPFL-LTE managed a mobile X-band polarimetric (MXPol) radar, which provided a combination of range height indicator (RHI) and PPI scans of polarimetric variables every 5 min. These two research radars enabled the monitoring of low-level precipitation over the Auzon catchment. Their maximum range should vary between 30 and 40 km (the range represented in Fig. 3a is only qualitative). Finally, five Micro Rain Radars (MRRs), provided by CNRM, LaMP and OSUG, were deployed in combination during the autumns of 2012 and 2013 at three locations in the region of interest to document the vertical profile of precipitation. These Doppler FW-CW vertically pointing radars measuring the Doppler spectra enable study of the vertical structure of rainfall as well as the associated microphysical processes in relation with the orography (Zwiebel et al., 2015). More detailed information about the operational and research radar systems involved in HyMeX can be found in Bousquet et al. (2015). The operational radar processing algorithms are described in Tabary (2007), while the data from the MXPol radar are processed following the steps described in Schneebeli et al. (2014) and Griazioli et al. (2015). The characteristics of MXPol are given by Schneebeli et al. (2013) and Mishra et al. (2016).

Disdrometers

A network of 16 OTT Parsivel disdrometers (optical spectro-pluviometers), 11 of which are of the first generation and 5 of the second generation, covers the southern part of the Auzon catchment (Figs. 3a and 4) and extends lightly more to the west, up to Saint-Etienne de Fontbellon, referred to as STEF in Fig. 3a. At least five devices were available at the same time from 15 November 2011 (see Table A2 in Appendix A for the period of operation of the instruments). Moreover, a 2-D video disdrometer (2-D VD) was deployed at Le Pradel

Table 1. Overview of the instruments used to gather the hydrometeorological variables in the region that encompasses the Auzon catchment (Ardèche, France) between 2011 and 2014. Note that RHI means "range height indicator", PPI means "plan position indicator", Op means "operational", and Res means "research". The column "Number" indicates the maximum number of instruments in operation at the same time.

Compartment	Op/res	Instrument	Variable	Unit	Number	Observation frequency	Integration method
Rainfall	Op	S-band Doppler and polarimetric radar	Reflectivity Cumulative rainfall	dBZ mm	2 2	5 min	Instantaneous
	Res	X-band Doppler and polarimetric radar (MXPol)	Horizontal reflectivity Differential reflectivity Differential phase Doppler power spectra Cross-spectra	dBZ dBZ ° dBm dBm	1 1 1 1 1	5 min Combination of RHI and PPI scans	Instantaneous
	Res	X-band fast-scanning radar (WR-10X+)	Reflectivity	dBZ	1	3 min	Instantaneous
	Res	Micro Rain Radar (MRR-2)	Reflectivity	dBZ	3	10 s resolution–1 min average	Integrated
	Res	Disdrometer (Parsivel 1)	Drop size distribution Drop velocity distribution Precipitation rate	$mm^{-1}\,m^{-3}$ $mm\,h^{-1}$	11 11 11	30 s or 1 min	Integrated
	Res	Disdrometer (Parsivel 2)	Drop size distribution Drop velocity distribution Precipitation rate	$mm^{-1}\,m^{-3}$ $mm\,h^{-1}$	5 5 5	1 min	Integrated
	Op	Rain gauge (Météo-France, SPC Grand Delta)	Cumulative rainfall	mm	10	1 h (Météo-France), 5 min (SPC)	Integrated
	Res	Rain gauge (Hpiconet) (R3039 1000 cm^2)	Cumulative rainfall	mm	20	5 min	Integrated
Meteorology	Op	Temperature probe (PT100)	Air temperature	°C	6	1 h	Instantaneous
	Res	Baro-Diver (DI500) Mini-Diver (DI501)	Air temperature Atmospheric pressure	°C cm H_2O	4 4	2 min 2 min	Instantaneous Instantaneous
	Op	Humidity probe (HMP45D)	Relative humidity	%RH	5	1 h	Instantaneous
	Op	Barometer (PTB220)	Atmospheric pressure	hPa	1	1 h	Instantaneous
	Op	Wind sensor (DEOLIA 96, Alizia 312)	Wind speed Wind direction	$m\,s^{-1}$ °	2 2	1 h 1 h	Instantaneous Instantaneous
	Op	Pyranometer (Kipp & Zonen Inc.)	Shortwave/longwave radiation	$W\,m^{-2}$	1	1 h	Instantaneous

Table 2. Overview of the instruments used to gather the hydrological and suspended sediment variables in the Auzon catchment (Ardèche, France) or its close vicinity between 2011 and 2014.

Compartment	Instrumental device	Instrument	Variable	Unit	Number	Location	Observation frequency
Surface water	Hydrometric stations	Pressure probe (PLS)	Water level	m	1	Gazel	2 min
			Discharge	$L\,s^{-1}$	1	Gazel	2 min
		Radar level sensor (Cruzoe)	Water level	m	1	Cladugne	10 min
			Discharge	$m^3\,s^{-1}$	1	Cladugne	10 min
		Radar level sensor (RLS)	Water level	m	1	Auzon	5 min or 1 h
			Discharge	$m^3\,s^{-1}$	1	Auzon	5 min or 1 h
		LSPIV/camera (VW-BP330)	Water surface velocity	$m\,s^{-1}$	1	Auzon	5 min or 1 h
		Radar surface velocity sensor (RG-30)	Water surface velocity	$m\,s^{-1}$	1	Cladugne	10 min
		Acoustic Doppler velocimeter (IQ Plus)	Water velocity profile	$m\,s^{-1}$	1	Cladugne	10 min
		Conductivity and temp. probe (CS547)	Water conductivity	$\mu S\,cm^{-1}$	2	Gaz., Cla.[f]	2 or 10 min
			Water temperature	°C	2	Gaz., Cla.[f]	2 or 10 min
		Suspended solids probe (Visolid IQ 700)	Turbidity	$g\,L^{-1}\,SiO_2$	2	Gaz., Cla.[f]	2 or 10 min
		3700 portable sampler	Sediment concentration	$g\,L^{-1}$	2	Gaz., Cla.[f]	10 or 40 min
	Water erosion plots	HS flume with level sensor (Thalimedes)	Discharge	$L\,s^{-1}$	2	Le Pradel	1 min
		3700 portable sampler	Sediment concentration	$g\,L^{-1}$	2	Le Pradel	variable
	Stream sensor network	Mini-Diver (DI501)	Water level	m	7	[a]	2 min
			Water temperature	°C	7	[a]	2 min
		CTD-Diver (DI271)	Water level	m	4	[b]	2 or 5 min
			Water temperature	°C	4	[b]	2 or 5 min
			Water conductivity	$\mu S\,cm^{-1}$	4	[b]	2 or 5 min
			Discharge	$L\,s^{-1}$	4	[b]	2 or 5 min
Soil	Soil moisture network	ThetaProbe	Soil volumetric water content	$m^3\,m^{-3}$	6 transects × 25 points	[c]	pre- and post-event
		10 HS	Soil volumetric water content	$m^3\,m^{-3}$	9 profiles with 5 sensors	[d]	20 min
		ThetaProbe (ML2X)	Soil volumetric water content	$m^3\,m^{-3}$	1 profile with 4 sensors	[e]	1 h
			Soil temperature	°C	1 profile with 4 sensors	[e]	1 h

[a] The group of stations represented by green stars in Fig. 3c (bz1, mi1, mi2, mi4, sg2, sj2, sj3).
[b] The group of stations represented by blue stars in Fig. 3c (sg1, sj1, mi3, vb1).
[c] The points represented by blue circles in Fig. 5.
[d] The points represented by red plus signs in Fig. 5.
[e] The points represented by a black cross in Fig. 5.
[f] Abbreviation for "Gazel, Cladugne".

(south of the Gazel catchment) in autumn 2012 and 2013 for an inter-comparison of measurements (Raupach and Berne, 2015). All Parsivels except Saint-Etienne de Fontbellon and Pradel-Grainage are colocated with rain gauges from the network described in the next paragraph (Fig. 4). The correction technique described by Raupach and Berne (2015) using the 2-D VD as a reference disdrometer has been applied to Parsivel data, improving the consistency of recorded drop size distribution (DSD) moments.

Rain gauges

An operational network of 10 rain gauges (6 managed by Météo-France and 4 managed by the Flood Forecasting Service – SPC Grand Delta) is present over the Auzon catchment or its close vicinity (Fig. 3a). It provides data at an hourly time step (Météo-France rain gauges) and 5 min time step (SPC Grand Delta rain gauges). Additionally, a research network of 21 rain gauges is implemented over the Auzon catchment (Fig. 3a). It provides data at 5 min time step. Nineteen rain gauges were initially deployed over a 7 km × 8 km area located in the southern part of the catchment (Fig. 4) and 2 additional rain gauges were subsequently installed in the northern part of the Claduègne catchment. This network, called Hpiconet, was designed for sampling rainfall at spatial scales ranging from tens of metres to tens of kilometres and at temporal scales ranging from 1 min to 1 day. This offers the opportunity to address the issues of the definition of the scales of variability in rainfall and the origins of this variability that are still open questions within the hydrometeorological community (Fraedrich et al., 1993; Fabry, 1996; Krajwesky et al., 2003). The rain gauges are distributed over 11 main locations with a mean interdistance of about 2 km. At some locations, several rain gauges are clustered with interdistances of 10 to 500 m as seen in the inset maps of Fig. 4. All rain gauges are identical and consist of a Précis Mécanique tipping bucket of 0.2 mm (model 3039) with a collecting area of 1000 cm^2. Each rain gauge is connected to a HOBO or Campbell data logger. A first step of the data quality control consists of comparing the total rain amount recorded by the tipping bucket–HOBO system with that collected at the outlet of the rain gauge with a 30 L plastic tank. The comparison of these two measurements shows that the relative difference remains below 10 % for all the rain gauges and lower than 5 % for most of them. Calibration is performed if an error of more than 5 % is detected. In a second step, the temporal evolution of cumulated sums of rainfall of close stations are plotted against each other. Clogged buckets never occurred thanks to the frequent maintenance (at least once a month).

3.1.2 Other meteorological data

Most of the meteorological variables originate from one of the operational surface observing networks of Météo-France. Six stations are located in the Auzon catchment or its close vicinity. All of them continuously provide hourly measurements. The measured variables at each station differ depending on the network to which each station belongs. There are four types of networks for Météo-France stations present in this study: the "aeronautical synoptic" network (including LANAS-SYN), the RADOME-RESOME network with automatic stations also known as the Automated Regional Network (including BERZEME-RAD), the network of automatic stations surveyed in real time (including ALBA-SA and ESCRINET) and the network of automatic stations examined in delayed time (including AUBENAS-SA et MIRABEL-SA). Each observing network has its own purposes, so the variables needed are different. For instance, LANAS-SYN is the only station that provides surface pressure. Figure 3b shows the location of each station together with the variables they measure.

Air temperature and relative humidity

Each of the six stations considered is equipped with a WMO-standard meteorological shelter, which is installed 1.5 m above ground. Both an air temperature sensor (PT100) and a relative humidity sensor are mounted in the shelter so that they are protected from solar radiation.

Atmospheric pressure

Atmospheric pressure is measured by a digital barometer (PTB220) at one of the six stations considered.

Wind speed and direction

Wind measurements are conventionally performed at 10 m above ground surface level and on open ground at three of the six stations considered. Wind speed is given by a cup anemometer, while wind direction is measured thanks to a vane mounted on a pole that has pointers indicating the principal points of the compass.

Global radiation

Several measurements of radiation can be performed. One out of the six considered stations is equipped with a pyranometer (CM11) providing global solar radiation values.

Additionally, one Baro-Diver and three Mini-Divers were deployed over the Claduègne catchment to complement the stream sensor network to measure the atmospheric pressure and the air temperature with an observation frequency of 2 min (Fig. 3b). However, these four sensors are not located in a shelter and are therefore subject to solar radiation.

3.2 Spatial characterization data

Characterization data are used to define the topography, pedology, geology, land use, landscape and hydrological

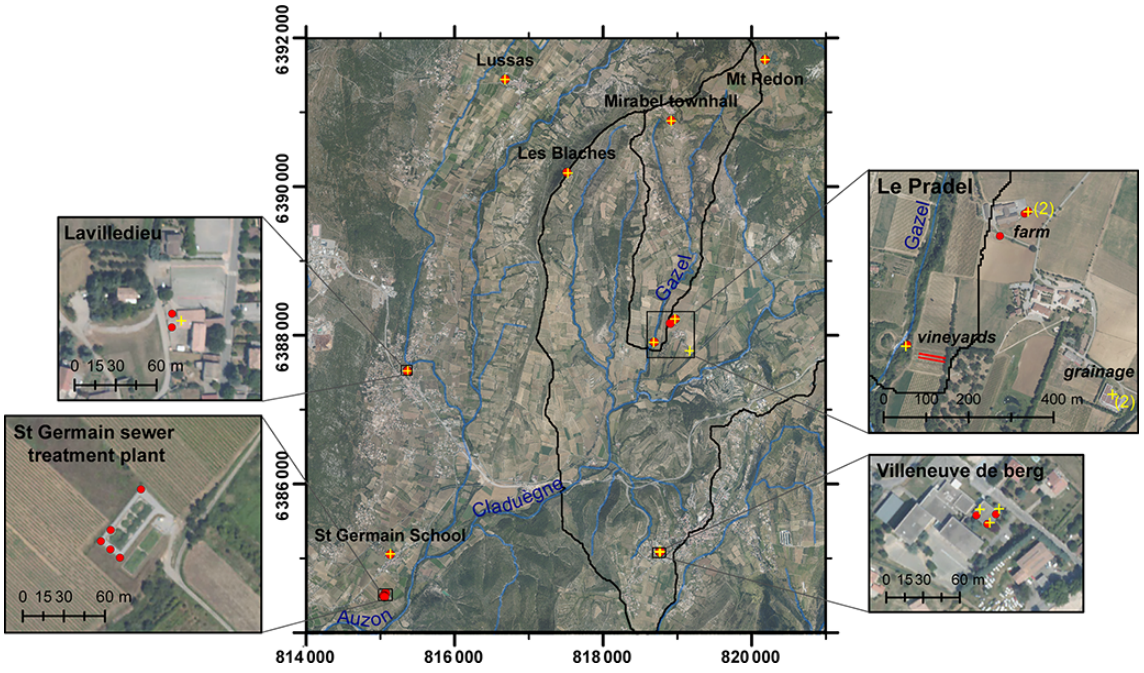

Figure 4. Location of the 19 Hpiconet rain gauges (red dots) and 14 disdrometers (yellow crosses) deployed over a 7 km × 8 km area in the southern part of the Auzon catchment. Where rain gauges are clustered with interdistances of 10 up to 500 m, inset maps present the configuration of the deployment at the local scale. The names of the location of the instruments are indicated in black. For the "Le Pradel" site, two sub-sites are indicated and the location of the soil erosion plots is represented with red lines. The boundaries of the Gazel and Cladueègne catchments are displayed in black. Orthophotos are displayed in the background (source: IGN France 2009).

properties of the Auzon catchment. These data provide the fine-scale detail required for modelling and hydrological assessment. The coordinate system of reference used in this study is the Réseau géodésique français (RGF) 1993 (official in France, based on IAG-GRS80 ellipsoid, very similar to WGS 84). The projection is Lambert conique conforme. Table 3 presents the main GIS descriptors available for the region of interest in this study.

3.2.1 GIS descriptors

For the Cladueègne catchment, a 1 m bare-earth digital elevation model (DEM) was derived from an aerial lidar dataset acquired in 2012 and processed by Sintégra (Braud et al., 2014). For the Auzon catchment, the 25 m DEM released by IGN France in 2008 is available. A combination of these two latter DEM was performed using ArcGis based on re-sampling and interpolation to produce a 5 m DEM over the Auzon catchment from which the catchment boundaries were derived using TAUDEM D8 incorporated in ArcGis. A map (scale 1 : 50 000) of the geology of the region including the Auzon catchment was released by the Bureau de Recherches Géologiques et Minières (BRGM) in 1996 and digitalized in vector format from 2001 (Elmi et al., 1996). A map (scale 1 : 100 000) of the pedology of the region including the Auzon catchment was released by INRA (Bornand et al., 1977). In addition, the Ardèche soil database at scale 1 : 250 000 produced by Sol-Conseil and Sol Info Rhône Alpes provides a vector map of the region synthesizing a large amount of information on soil (soil class and unit, horizon, thickness, etc.) and bedrock. Very high resolution images were acquired and processed to provide detailed land use maps: 5 m resolution satellite images (QuickBird images) taken in 2012 for the Cladueègne catchment and 30 m resolution satellite images (Landsat) taken in 2013 for the Ardèche catchment. The orthophotography database released by IGN France in 2009 provides aerial images of the Auzon catchment at a resolution of 0.5 m. In addition, vector data of the drainage network, catchment boundaries, instrument locations, administrative boundaries and road network are available.

3.2.2 Infiltration tests

A field campaign aiming at documenting the variability in surface hydraulic properties was conducted in May–June 2012 in the Cladueègne catchment. The measurements were performed at 17 points throughout the catchment (Fig. 5), which were selected from the cross-analysis of pedology, land cover and geology maps following the method of Gonzalez-Sosa et al. (2010). The tested hypothesis is that land use has a major influence on the observed hydraulic properties rather than the soil texture. Two techniques were used: the mini disk infiltrometer and the double-ring infiltrometer using the Beerkan method (Braud et al., 2005). With

the exception of two points, both instruments were used at each location. Between one and three repeated measurements were performed. Soil texture was then analyzed at the INRA laboratory of soil analyses in Arras (France). The results of this campaign are described in Braud and Vandervaere (2015).

3.3 Hydrological and sediment data

Almost all the instruments deployed in the field to measure the soil and surface water compartments were installed for research purposes. There was virtually no hydrological observation before 2011 in the Auzon catchment, except the water erosion plots and a site for soil moisture measurement (SMOSMANIA network). Most of the instruments were installed in the framework of the FloodScale project and the HyMeX EOP (2011–2014). The instruments are located mainly in the Gazel and Claduègne sub-catchments (Fig. 3c), where it was decided to put the major efforts.

3.3.1 Surface water

Hydrometric stations

Three hydrometric stations with natural controls are located respectively on the Gazel, Claduègne and Auzon rivers (Fig. 3c). The Claduègne and Auzon stations are situated at a bridge in order to facilitate the access and the manipulations during floods; they were installed respectively in October 2011 and June 2013. Water level is measured using H radar (Table 2). The Gazel station is situated on a natural reach without any construction; it was installed in April 2011. Water depth is measured using a hydrostatic pressure probe. The common variables provided by these three stations are water level and stream discharge. The observation frequency is respectively 2, 10, and 5 min for the Gazel, Claduègne and Auzon stations. The logged values are time-averaged measurements (typically 30 values over less than 1 min), with their dispersion (standard deviation, minimum and maximum values). A significant effort was dedicated to the establishment of the stage–discharge relationships during the period 2012–2014. Many on-alert campaigns were carried out to perform discharge measurements at high flows. All the discharge measurements with their estimated uncertainties at the 95 % level of confidence are presented in Table 4. Different techniques and instruments, including salt dilution, current meter, surface velocity radar (SVR) (Welber et al., 2016), acoustic Doppler current profiler (ADCP), acoustic Doppler velocimeter (ADV) and large-scale particle image velocimetry (LSPIV), based on images recorded by a fixed camera (Le Coz et al., 2010; Dramais et al., 2015), were used depending on the type of river and the hydraulic conditions. The BaRatin framework (Le Coz et al., 2014) combining Bayesian inference and hydraulic analysis was used to build steady, multi-segment stage–discharge relationships

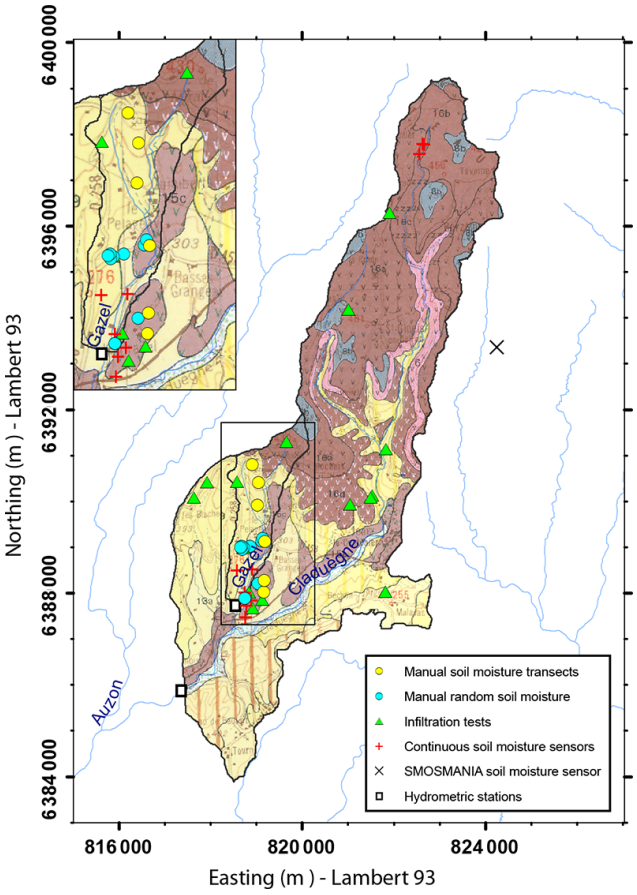

Figure 5. Location of infiltration tests and soil moisture measurements in the Gazel and Claduègne catchments. The soil moisture measurements include both manual and continuous measurements. The black rectangle shows the position of the zoom provided at the top left of the figure. The pedology (1 : 100 000 soil map; source: INRA) is displayed in the background.

and to estimate the associated uncertainty (95 % confidence interval).

Additional variables are provided by these stations. At the Gazel and Claduègne stations, different physico-chemical variables of the surface water are measured continuously: temperature, conductivity and turbidity. Generally, for all inter-flood periods (marked by very low turbidity) the turbidity value was set to 0 during the procedure of data quality control even if there was a value different from 0 in the raw data. Indeed, the turbidimeters used in this study are designed for a high turbidity range (typically 1000 to 10 000 ppm) and are not capable of accurately measuring low turbidity (typically less than 50 ppm). Sequential samplers, triggered by the data logger, collect water and suspended sediment samples when threshold values of water level and turbidity are exceeded. The suspended sediment concentration (SSC), which represents the mass of solid divided by the volume of liquid (expressed in $g\,L^{-1}$), is estimated by measuring the volume

Table 3. List of GIS descriptors available for the Auzon catchment.

GIS descriptor	Data	Type	Date	Legend	Author	Access
Topography	1 m bare-earth DTM[a] of Claduègne catchment	Raster	2012	Lidar campaign	Sintégra géomètres experts	Public
	25 m bare-earth DTM of Auzon catchment	Raster	2008	BD TOPO, Ardèche	IGN France	Marketed product[c]
	5 m bare-earth DTM of Auzon catchment	Raster	2014	Combination of data based on resampling and interpolation	IGE	Public
Geology	Map of Auzon catchment at scale 1 : 50000	Vector	1996	BD Charm-50, Aubenas	BRGM	Marketed product[c]
Pedology	Map of Auzon catchment at scale 1 : 100000	Raster	1977	Pedological map of France at 1 : 100000, Privas	INRA	Marketed product[c]
	Map of Auzon catchment at scale 1 : 250000	Vector	2001	IGCS – Référentiel Régional Pédologique, BDSol-Ardèche	BRGM/Chambre Agriculture	Marketed product[c]
Soil properties	Soil depth for each SCU[b]	Vector	2015	Processed from the Ardèche soil database at 1 : 100000	IRSTEA Lyon	Public
	Maximum soil water storage for each SCU	Vector	2015	Processed from the Ardèche soil database at 1 : 100000	IRSTEA Lyon	Public
	Soil texture of superficial layer for each SCU	Vector	2015	Processed from the Ardèche soil database at 1 : 100000	IRSTEA Lyon	Public
	Soil stone content for each SCU	Vector	2015	Processed from the Ardèche soil database at 1 : 100000	IRSTEA Lyon	Public
Infiltration tests	Infiltration campaign Claduègne catchment	Vector	2012	52 sampled points	IRSTEA Lyon	Public
Land use	5 m resolution images of Claduègne catchment	Vector/raster	2012	Processed from QuickBird images	UMR Espace	Public
	30 m resolution images of Auzon catchment	Raster	2013	Processed from Landsat images	UMR Espace	Public
Orthophotography	0.5 m resolution images of Auzon catchment	Raster	2009	BD ORTHO, Ardèche	IGN France	Marketed product[c]
Surface information	Catchment boundaries	Vector	2014	Processed from the 5 m bare-earth DEM with TAUDEM D8 tool	IGE	Public
	Drainage network (stream)	Vector	2010	BD CARTHAGE	Sandre eaufrance	Public
	Drainage network (permanent and intermittent)	Vector	2008	BD TOPO, Ardèche	IGN France	Marketed product[c]
	Instruments	Vector	2014	Point	IGE	Public
	Road network	Vector	2008	BD TOPO, Ardèche	IGN France	Marketed product[c]
	Administrative boundaries	Vector	2008	BD TOPO, Ardèche	IGN France	Marketed product[c]

[a] DTM: digital terrain model.
[b] SCU: soil cartographic unit.
[c] Not released in this study.

Table 4. List of the discharge measurements carried out at three hydrometric stations (Gazel, Cladugne, Auzon) between 2011 and 2014. The gauging techniques/instruments include salt dilution, current meter, surface velocity radar (SVR), acoustic Doppler current profiler (ADCP), acoustic Doppler velocimeter (ADV), large-scale particle image velocimetry (LSPIV), and Manning–Strickler.

Hydrometric station	Date	Stage	Discharge (95 % confidence level)	Expanded uncertainty	Method
	(UTC)	(cm)	($L s^{-1}$)	(%)	
Gazel	08/11/2011 11:03	11.5	240.4	10	Salt dilution
	08/11/2011 11:09	11.4	216.4	10	Salt dilution
	05/01/2012 14:22	−8.7	4.7	7	Salt dilution
	05/01/2012 14:26	−8.7	4.7	7	Salt dilution
	17/02/2012 13:43	−10.2	2.7	7	Salt dilution
	17/02/2012 13:46	−10.2	2.7	7	Salt dilution
	01/03/2012 14:23	−10.6	2.0	7	Salt dilution
	01/03/2012 14:27	−10.6	2.1	7	Salt dilution
	08/03/2012 16:28	−10.4	1.8	7	Salt dilution
	08/03/2012 16:33	−10.4	1.8	7	Salt dilution
	27/11/2012 06:50	12.5	210.0	7	Salt dilution
	13/03/2013 14:55	0.5	41.9	7	Salt dilution
	13/03/2013 14:55	0.5	40.9	7	Salt dilution
	17/04/2013 14:40	−3.5	15.1	10	Salt dilution
	17/04/2013 14:40	−3.5	15.4	10	Salt dilution
	23/10/2013 11:00	31	1026	5	Salt dilution
	23/10/2013 13:35	74.5	8000	25	SVR
	18/02/2014 15:00	4.5	105.0	20	Salt dilution
	13/10/2014 08:20	7	169.0	5	Salt dilution
Cladugne	01/03/2012 12:45	22.9	71.3	10	Salt dilution
	01/03/2012 12:50	22.9	71.6	10	Salt dilution
	08/03/2012 12:40	22.5	72.2	10	Salt dilution
	08/03/2012 12:45	22.5	69.6	10	Salt dilution
	06/09/2012 10:00	19.35	42.6	10	Current meter
	10/11/2012 07:53	107	17 580	20	SVR
	27/11/2012 08:40	78.5	7670	15	SVR
	17/04/2013 13:30	35	229.3	10	Salt dilution
	17/04/2013 13:30	35	245.6	10	Salt dilution
	13/05/2013 16:25	41	438.4	10	Salt dilution
	13/05/2013 16:30	41	435.5	10	Salt dilution
	31/07/2013 14:00	25.5	172.0	10	Current meter
	23/10/2013 14:40	180	50 750	20	SVR
	13/11/2013 14:10	30.5	298.0	12	Salt dilution
	20/09/2014 06:48	73	5970	15	SVR
	10/10/2014 10:00	67	3000	30	ADCP
	11/10/2014 06:20	99	11 890	20	SVR
	13/10/2014 10:50	60	1953	15	Current meter
	13/10/2014 14:10	137.5	27 800	15	SVR
	13/10/2014 15:20	121.5	20 710	15	SVR
	04/11/2014 07:30	242.5	95 190	20	SVR
	04/11/2014 09:40	159	36 650	20	SVR
	04/11/2014 14:10	340	204 000	25	SVR

of liquid present initially in the sample and weighting the solid fraction after drying it at 105 °C. The detailed procedure was given by Navratil et al. (2011) and resulted in a median relative uncertainty of 15 %. Some selected samples are analysed using a laser diffraction particle size analyser (Malvern Mastersizer/E) to characterize the particle size distribution. At the Cladugne station, water surface velocity is measured continuously using the non-contact radar technology based on the principle of the frequency shift due to the Doppler effect. The continuous measurement of water velocity has become increasingly common in the US and in Europe, especially for operational hydrometric agencies, as it

Table 4. Continued.

Hydrometric station	Date	Stage	Discharge (95 % confidence level)	Expanded uncertainty	Method
	(TU)	(cm)	($L s^{-1}$)	(%)	
Auzon	22/05/2013 14:15	21	1520	15	ADCP
	23/10/2013 11:39	125	27 900	15	SVR
	23/10/2013 12:21	125	34 700	15	SVR
	23/10/2013 12:25	130	55 300	15	SVR
	04/01/2014 10:46	153	68 480	15	LSPIV
	19/01/2014 00:00	170	280 000	15	Manning–Strickler (IPEC)
	19/01/2014 15:26	121	48 480	15	LSPIV
	05/02/2014 11:16	85	29 120	15	LSPIV
	06/02/2014 13:30	43	8030	5	ADV
	20/09/2014 07:01	54	14 915	15	LSPIV
	11/10/2014 07:55	75	18 400	15	SVR
	13/10/2014 13:35	30	2660	10	ADV
	20/10/2014 05:37	55	12 200	15	SVR
	04/11/2014 06:21	177	86 080	15	LSPIV
	04/11/2014 07:07	255	162 000	15	SVR
	04/11/2014 08:31	282	169 148	15	LSPIV
	04/11/2014 08:50	245	125 000	15	SVR
	04/11/2014 09:01	261	146 269	15	LSPIV
	04/11/2014 09:31	210	113 968	15	LSPIV
	04/11/2014 09:55	180	846 00	15	SVR
	04/11/2014 14:31	343	228 860	15	LSPIV
	04/11/2014 14:35	300	247 000	15	SVR
	04/11/2014 14:36	350	226 000	15	SVR
	04/11/2014 15:05	365	257 000	15	SVR
	04/11/2014 15:21	381	296 570	15	LSPIV
	04/11/2014 16:21	317	206 310	15	LSPIV
	14/11/2014 07:25	90	29 200	15	SVR
	15/11/2014 06:31	103	38 491	15	LSPIV

allows for the index velocity method to be applied (Levesque and Oberg, 2012). This approach is particularly relevant to small rivers subject to flash floods where flow is highly unsteady. It represents a useful tool for extrapolating stage–discharge rating curves over a range of flows for which the use of conventional gauging methods is impractical or unsafe (Nord et al., 2014). At the Claduègne station, an acoustic Doppler velocity meter was fixed to the channel bed during the period from September 2013 to November 2014 to measure detailed velocity profile (100 cell maximum) at the same observation frequency as water level and surface velocity. This system provides an alternative continuous measurement of flow velocity in the water column from the bed up to the water surface.

Overland flow and water erosion

Two erosion plots were monitored on a hillslope with vineyard at "Le Pradel" (Figs. 2e and 4) during the period from December 2009 to October 2013. The erosion plots, considered as two duplicates, are 60 m long and 2.2 m wide and they extend over the entire length of the hillslope. The width of the plots corresponds to the distance between two vine rows oriented in the direction of the main slope. The vine rows are located on the edges of each plot. The two plots are parallel and spaced by approximately 5 m. The average slope in the longitudinal direction is about 15 %. The vegetation cover between the vine rows varied between years but remained very sparse. The brown calcareous soils underlain by marly limestones are composed of 34 % of clay, 41 % of silt and 25 % of sand particles. The Gazel River is located about 40 m away from the monitored hill foot. The transition between the cultivated hillslope and the river is marked by a riparian vegetation zone and a cliff of about 10 m. This monitored hillslope is included in the catchment, whose outlet corresponds to the Gazel hydrometric station, with the idea of investigating the fate of solid particles eroded from the hillslope to the river.

A rain gauge and a disdrometer were located at about 30 m from the erosion plots (Fig. 4). The two plots were equipped similarly. Runoff was collected in the bottom part of the hillslope. The water depth was measured every minute with a

1 mm resolution using a gauge (OTT Thalimedes) within an H flume designed following the US Soil Conservation Service recommendations. The stage–discharge rating curve was built experimentally and allowed for calculation of discharge with a median relative uncertainty of 10 %. A sequential sampler containing 24 bottles of 1 L capacity sampled water and eroded particles within the H flume. When critical thresholds of water depth or water depth variation were exceeded, the data logger triggered the sampling of water and eroded particles. Thus, the time intervals between each two samples were irregular, depending on the shape of the hydrograph. SSC were estimated following the procedure given above in the section "Hydrometric stations". While the discharges were available continuously, the sediment fluxes were only calculated for the times where SSC values were available. Many samples were analysed using a laser diffraction particle size analyser (Malvern Mastersizer/E) to characterize the particle size distribution. More details about the description of the plots, the topographical data available, and the monitored runoff and erosion events are given by Grangeon (2012) and Cea et al. (2016). The infiltration and runoff processes over this hillslope were previously studied by Nicolas (2010).

Stream sensor network

A stream sensor network composed of four CTD-Divers (conductivity–temperature–depth) and seven Mini-Divers (temperature–depth) was deployed on the Gazel and Claduègne catchments (Fig. 3c). These compact instruments (Table 2) for autonomous measurement and record were installed in small metallic boxes (177 mm × 81 mm × 57 mm) embedded in the riverbed in the case of bedrock rivers and anchored vertically to the wall or any other fixed element in the rest of cases. The lids of the boxes were perforated to ensure water permeability. In addition, in the case of the CTD-Divers, a hole of 3 cm in diameter was formed at each end of the boxes to let the water circulate and ensure a significant renewal of water inside. The instruments were installed in the intermittent hydrographic network, delineating 10 sub-catchments of 0.17–2.2 km^2 and one sub-catchment of 12.2 km^2, which contains the whole area with volcanic geology of the upstream part of the Claduègne catchment. The selected sites are mainly headwater sub-catchments where the landscape properties are considered homogeneous in terms of geology, pedology and land use (Fig. 3). The underlying assumption in the choice of the measurement sites was that the delineated sub-catchments were homogeneous hydrological units and could lead to different responses for the same rainfall forcing. Taken together, these selected sub-catchments constituted a representative sample of the landscapes encountered in the Gazel and Claduègne catchments. Given that rainfall is highly variable in space and time in this region, the observation system enables assessment of the hydrological response to rainfall fields.

The CTD-Divers and Mini-Divers measure the total pressure as they are not compensated for (cableless instruments). An independent measurement of atmospheric pressure is therefore necessary for accurate barometric compensation and consecutive calculation of the hydrostatic pressure or water depth. Initially (in September 2012), only one barometer (a Baro-Diver) was installed in the area following the manufacturer's recommendation, which specifies that, in general, in relatively flat open terrain, the pressure measurement has a maximum range of 15 km. However, the error in the measurement of water level was important in our case (about 2 cm), mainly due to the error in the atmospheric pressure which varies significantly throughout the area due to the relief and the differences in climate between the Coiron Plateau and the piedmont hills. As a consequence, three additional Mini-Divers (used as barometers) were progressively deployed from November 2012 to April 2013 in the Gazel and Claduègne catchments to reduce the measurement error of water level to about 1 cm. In order to compensate for the total pressure values measured by the CTD-Divers and Mini-Divers, it is necessary to calculate the atmospheric pressure at all points of the stream sensor network. For this, we rely on the four points of atmospheric pressure measurement available and we choose between the following two options according to criteria of distance and difference of altitude between the calculated point and the measuring points:

1. linear interpolation of atmospheric pressure between the two closest points of measurement based on the difference of altitude with the calculated point;

2. meteorological method of correcting pressure (National Advisory Committee for Aeronautics, 1954) based on the nearest point of pressure and temperature measurement by applying a standard temperature gradient ($-6.5\,K\,km^{-1}$).

The results are not very sensitive to the method used, with the most sensitive factor being the density of atmospheric pressure measurement over the spatial extension of the stream sensor network.

When possible, controlled sections are chosen to allow the establishment of a stage–discharge relationship based on stability and sensitivity of the control points. This is the case for three points of the stream sensor networks: mi3, sj1, and vb1 (Fig. 3c). Mi3 is located on a concrete, broad-crested artificial control, sj1 on a natural weir and vb1 in a circular concrete culvert. Many on-alert campaigns were carried out to perform discharge measurements at different flow conditions at these points and at two additional points (bz1 and sg1) for which stage–discharge relationships could be established in the future.

3.3.2 Soil

Soil moisture

Infiltration excess runoff was thought to be the dominant process (e.g. Nicolas, 2010) in the Gazel and Claduègne catchments. The observation strategy thus focuses on the documentation of the soil infiltration capacity and initiation of ponded conditions at the surface. The monitoring of soil moisture in the Gazel and Claduègne catchments is a task that has two components:

1. mobile (manual) soil moisture measurements at the surface before/after rainfall events (good areal representativity);
2. deployment and maintenance of fixed sensors (continuous monitoring but point values).

A series of mobile soil moisture measurements were conducted in the Gazel catchment during HyMeX SOP1 (Huza et al., 2014). The measurements were taken on six fields, distributed over the whole catchment (Fig. 5). Fields were selected to appropriately represent the catchment, while still capturing inter-field variability and the influence of different topographical features. Vineyards were not selected because the soil was dominated by stones, making it impossible to sample without breaking the sensor. This resulted in all selected fields being pastures and grasslands. Within each of the selected six fields, a transect path of 50 m was measured. Along the 50 m transects, a measurement was taken at spatial intervals of 2 m and all measurements were done at the same location for each of the measurement days. Point volumetric soil moisture measurements were done using a portable three-prong (6 cm rod length) ThetaProbe ML2X sensor (Delta-T Devices Ltd, Cambridge, UK), which employs the frequency domain reflectometry (FDR) technique, and the internal default conversion tables (to convert output voltage to volumetric soil moisture content) were used. On each measurement day, all fields were measured within a few hours to minimize the influence of evaporation and drainage processes. The strategy was to select measurements days that aligned with high-precipitation events and to capture both pre-event and post-event soil moisture conditions whenever possible. During SOP1, 16 measurement days were completed on the six different transects. This produced approximately 2500 soil moisture measurements. The accuracy given by the manufacturer is $\pm 0.01\ \mathrm{cm^3\ cm^{-3}}$.

Nine sites (Figs. 3 and 5) with different land uses (two vineyards, four pastures, one piece of fallow land, two small oak woods) were selected for the installation of fixed sensors. Three sites are located in the Gazel catchment (two in the mi3 and one in the mi4 sub-catchments), three other sites are located in its close vicinity, and all are representative of the piedmont hills landscapes (Fig. 2d and e). The three last sites are located in the bz1 sub-catchment or its close vicinity and are representative of the Coiron Plateau landscapes (Fig. 2a). These choices of localization were motivated by the presence of the stream sensor network with the objective to make the most direct connection possible between rainfall forcing and hydrological response in small catchments relatively homogeneous in terms of geology and land use. The nine sites were equipped in 2013 with five sensors for continuous soil moisture measurements – two at about 10 cm, two at 20–25 cm and one at 30–50 cm depth – in order to document soil saturation (Braud et al., 2014). These five sensors are connected to the same data logger and the observation frequency is 20 min (Nicoud, 2015; Uber, 2016). The selected sensors are capacitive probes (Decagon 10 HS) which employ the FDR technique, and the internal default conversion tables (to convert output voltage to volumetric soil moisture content) were used. The range of volumetric soil moisture content of the instrument is between 0 and $0.57\ \mathrm{cm^3\ cm^{-3}}$ and the accuracy is $\pm 0.03\ \mathrm{cm^3\ cm^{-3}}$ according to the manufacturer.

Additionally, a station of SMOSMANIA (Soil Moisture Observing System – Meteorological Automatic Network Integrated Application) is located in the close vicinity of the upstream part of the Claduègne catchment, on the Coiron Plateau (Figs. 3c and 5). SMOSMANIA is based on the existing network of operational weather stations of Météo-France (RADOME). Among the 21 stations of this network that compose an Atlantic–Mediterranean transect in the southern part of France, Berzème is the station of interest for this study. The land cover around the station consists of fallow, cut once or twice a year. Four probes measuring soil moisture (ThetaProbe ML2X) were installed at the following depths: 5, 10, 20 and 30 cm.

Soil temperature

Soil temperature is measured at the station of SMOSMANIA (Berzème) at the following depths: 5, 10, 20 and 30 cm. The accuracy is $\pm 0.5\ ^\circ\mathrm{C}$.

4 First applications using the dataset

4.1 Areal rainfall estimation

Areal rainfall estimations are important for water budget assessment and the understanding of the internal catchment behaviour. Geostatistical techniques (rain gauge ordinary kriging, as well as merging of radar and rain gauge data through kriging with external drift) were used to obtain quantitative precipitation estimates (QPEs). The uncertainty of these QPEs was calculated using the methodology presented by Delrieu et al. (2014). The QPEs were produced for a wide range of spatial and temporal resolutions (15–360 min, 1–300 $\mathrm{km^2}$) for a 30 km × 32 km window encompassing the Auzon catchment in order to assess the effect of adding high-resolution rainfall data on the quality of the QPE for small scale hydrology applications. Rainfall estimates and error structure were compared for four scenarios with varying rain-

fall datasets (operational rain gauges, operational + research rain gauges, operational rain gauges + radar, all data) for the 25 largest rainfall events of 2012 and 2013. For all the scenarios, the results show that the error of the QPE increases with higher spatio-temporal resolutions. For the technique of kriging with external drift (merging radar and rain gauge data), there is a significant reduction in QPE error compared to the technique of ordinary kriging (using only rain gauge data), and this reduction is still more sensitive at higher spatio-temporal resolutions. Taking into account the data of the research rain gauge network (dense rainfall data) results in a reduction in QPE error. This reduction is similar to the decrease when adding the radar data; however, the spatial structure of the errors and the rainfall estimates of these scenarios show large differences.

Additionally, significant effort has been dedicated to the production of rainfall re-analysis (QPE) for the 2007–2014 period (Boudevillain et al., 2016) based on the operational radar and rain gauge data for a window of 32 000 km^2 including the major catchments of the Cévennes region (Doux, Eyrieux, Cance, Ardèche, Cèze, Gardons, Vidourle, Hérault). These QPEs were produced with a daily and hourly time resolution and for two types of geographic discretization: (1) Cartesian meshes of 1 km^2 for a regular grid covering the study area and (2) "hydrological" units corresponding to the discretization of the major catchments in subcatchments of homogeneous size in the range of 5, 10, 50, 100, 200, and 300 km^2. The uncertainty of these QPEs was also calculated using the methodology presented by Delrieu et al. (2014). An example of these QPEs is shown in Fig. 6 for the region of the Auzon catchment during the 4 November 2014 event between 13:00 and 14:00 UTC, which corresponds to the peak of rainfall preceding the peak of discharge measured at the Auzon station (Fig. 8). Figure 6a and b illustrate the added value of radar data to capture the spatial structure of rainfall even if, as for this case study (Fig. 6c and d), QPE error standard deviation may be sometimes larger than for ordinary kriging. Boudevillain et al. (2016) showed that, in general, QPE errors are significantly reduced with the technique of kriging with external drift. The data presented in this section are made available in the public dataset associated with this paper.

4.2 Improvement in the quantification of flood hydrographs and reduction of their uncertainty

The Gazel–Claduègne–Auzon experimental data were also used to develop a methodology to quantify and reduce the uncertainty of flood hydrographs. This methodology is based on the non-contact stream gaugings performed during the on-alert campaigns (see "Hydrometric stations" in Sect. 3.3.1) and on the BaRatin framework (Le Coz et al., 2014). At the Auzon hydrometric station, during the 2014 campaign, 11 LSPIV gaugings could be performed through the automated station. They were completed by 10 SVR gaugings. These

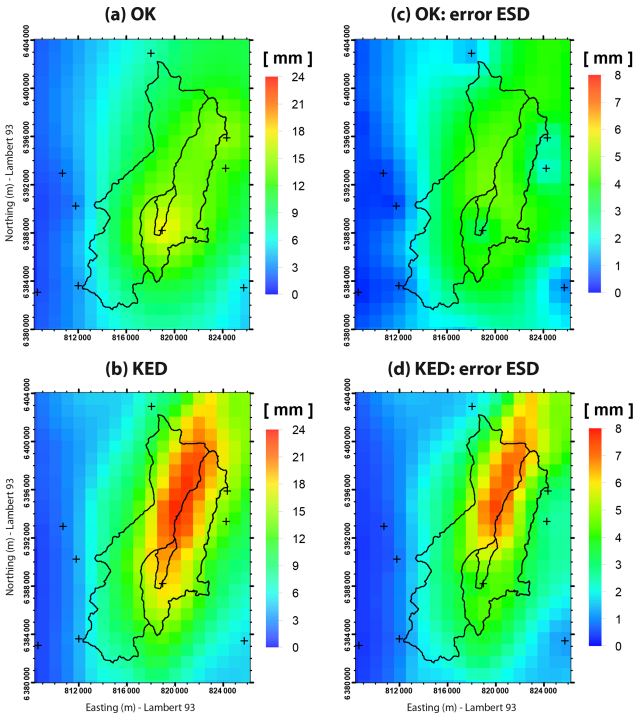

Figure 6. Ordinary kriging (OK) estimates from the operational rain gauge network (top) and kriging with external drift (KED) estimates from radar–operational rain gauge merging (bottom) for 4 November 2014 between 13:00 and 14:00 UTC. The graphs on the left display the estimation of hourly rain amounts (mm) and the graphs on the right display the corresponding error standard deviations (mm). The results are provided for a raster grid of 1 km^2 resolution.

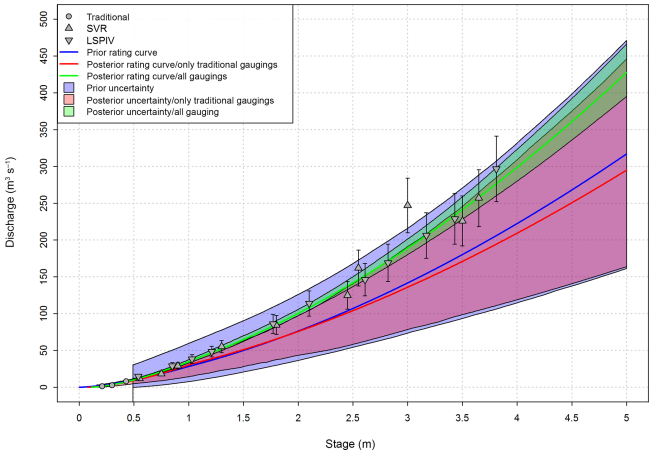

Figure 7. Stage–discharge rating curves and their uncertainty for the Auzon station: blue, prior rating curve based on hydraulic analysis only (no gaugings); red, rating curve established with traditional gaugings only; green, rating curve established with all gaugings, including high-flow non-contact gaugings. Solid lines represent the rating curves. Shaded areas represent the corresponding uncertainty 95 % confidence intervals.

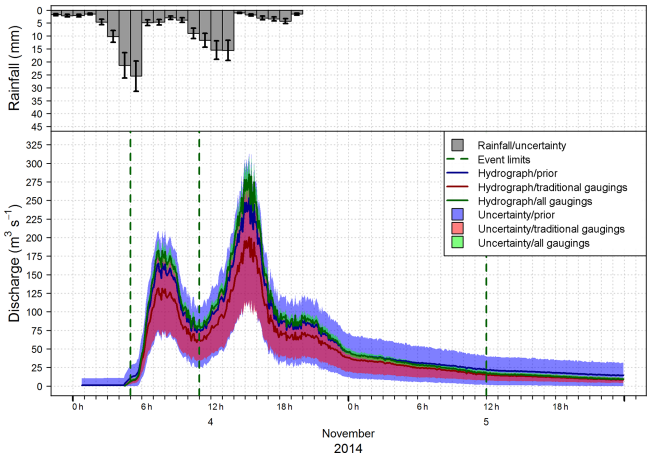

Figure 8. Event of 4 November 2014 on the Auzon catchment – hydrograph and associated uncertainty: blue, with prior rating curve (no gaugings); red, with rating curve established with traditional gaugings only; green, with rating curve established with all gaugings. Solid lines represent the hydrographs. Shaded areas represent the corresponding uncertainty 95 % confidence intervals.

gaugings have higher uncertainties than the traditional dilution or velocity–area methods, but have the advantage of being feasible safely even under hazardous, high flow conditions. These gaugings were incorporated as observations in the BaRatin methodology, which was further developed by adding the propagation of stage uncertainty and rating curve uncertainty to discharge time series (Horner, 2014; Branger et al., 2015). BaRatin is based on hydraulic analysis of the flow conditions at the stations, which are used as priors. The Bayesian framework then calculates the posterior rating curve and its associated uncertainty by incorporating the uncertain gaugings. Figure 7 shows that for the Auzon station, the new gaugings contributed to establish a rating curve significantly different from the prior rating curve, and different from the one which could have been obtained using traditional gauging methods only. The difference is particularly important for high flow. The rating curve uncertainty is also significantly reduced. Figure 8 shows the hydrograph and the associated uncertainty for the different rating curves presented in Fig. 7 for the 4 November 2014 event, the largest flood recorded during the period 2011–2014. The estimation of the flow volume during the event is 24 % underestimated without the non-contact gaugings. This improved accuracy in peak discharge and flow volume estimation is valuable not only for the validation of hydrological models but also for more applied purposes (flood forecasting, mapping of flood risk areas, water resources), along with estimation of rainfall uncertainty.

4.3 Distributed physically based soil erosion modelling

The impact of model simplifications on soil erosion predictions was tested by applying the GLUE methodology to a distributed event-based model at the hillslope scale (Cea et al., 2016). In this paper the authors analysed how the performance and calibration of a distributed event-based soil erosion model at the hillslope scale is affected by different simplifications on the parameterizations used to compute the production of suspended sediment by rainfall and runoff. Six modelling scenarios of different complexity were used to evaluate the temporal variability in the sediment flux at the outlet of a 60 m long cultivated hillslope. The six scenarios were calibrated within the GLUE framework in order to account for parameter uncertainty, and their performance was evaluated against experimental data registered during five storm events. The Nash–Sutcliffe efficiency (NSE), the percent bias (PBIAS) and coverage performance ratios showed that the sedimentary response of the hillslope in terms of mass flux of eroded soil can be efficiently captured by a model structure including only two soil erodibility parameters which control the rainfall and runoff production of suspended sediment. Increasing the number of parameters makes the calibration process more complex without increasing the predictive capability of the model in a noticeable manner.

5 Data availability

As an example of the kind of data made available in this paper, Fig. B1 in Appendix B shows an overview of rainfall, discharge and turbidity for the entire record (period 2011–2014) at the Claduègne hydrometric station. The measurement period is characterized by a wide variety of water conditions: a dry year in 2012, a wet year in 2014 and an intermediate year in 2013, as well as some intense rainfall events in spring 2013, autumn–winter 2013–2014 and autumn 2014. Note that the 4 November 2014 flood is a 5–10-year return period flood for the Claduègne River (this return period was roughly estimated from archive photos and interviews with residents and farmers who live and work near the river).

All the public datasets presented in this study are listed in Tables 5 and 6. In addition, all the datasets under the "associated scientists" status of the HyMeX data policy (http://mistrals.sedoo.fr/HyMeX/Data-Policy/HyMeX_DataPolicy.pdf) presented in this study are listed in Table 7. Data collected by a specific instrument and a network of instruments are listed in Tables 5 and 7, while the GIS descriptors are listed in Table 6. This granularity, also chosen for the DOI attribution (see the column "DOI" in Tables 5, 6, and 7), enables each individual dataset to be associated with a principal investigator who is very familiar with the data and who will be an essential resource for any user in case of need. The added-value dataset corresponding to the results of the rainfall re-analysis (QPE) for the

Table 5. Overview of the URL links and DOIs that allow for access to the public datasets presented in this study. The datasets are organized by instrument.

Compartment	Instrumental device/ instrument	Op/Res	Dataset name		Mistral data access	Status within Mistrals/HyMeX database[b]	DOI	Included in bundled data[c]
Rainfall	X-band Doppler and polarimetric radar (MXPol)	Res	MXPol-EPFL-LTERadar		http://mistrals.sedoo.fr/?editDatsId=721	Public after registration	doi:10.14768/MISTRALS-HYMEX.721	no
	X-band fast-scanning radar (WR-10X+)	Res	Le Chade LaMP X Band radar		http://mistrals.sedoo.fr/?editDatsId=796	Public after registration	doi:10.14768/MISTRALS-HYMEX.796	no
	Micro Rain Radar (MRR-2)		Micro Rain Radar LaMP Le Pradel		http://mistrals.sedoo.fr/?editDatsId=855	Public after registration	doi:10.14768/MISTRALS-HYMEX.855	no
			Micro Rain Radar LaMP St-Étienne-de-Fontbellon		http://mistrals.sedoo.fr/?editDatsId=1112	Public after registration	doi:10.14768/MISTRALS-HYMEX.1112	no
			Micro Rain Radar OSUG St-Etienne-de-Fontbellon		http://mistrals.sedoo.fr/?editDatsId=1158	Public after registration	doi:10.14768/MISTRALS-HYMEX.1158	no
			Micro Rain Radar OSUG Montbrun		http://mistrals.sedoo.fr/?editDatsId=1159	Public after registration	doi:10.14768/MISTRALS-HYMEX.1159	no
	Disdrometer (Parsivel 1)	Res	DSD network, Pradel-Vignes	[a]	http://mistrals.sedoo.fr/?editDatsId=436	Public after registration	doi:10.17178/OHMCV.DSD.PVI.11-14.1	zip1
			DSD network, Mont-Redon	[a]	http://mistrals.sedoo.fr/?editDatsId=679	Public after registration	doi:10.17178/OHMCV.DSD.MRE.12-14.1	zip1
			DSD network, Pradel-Grainage		http://mistrals.sedoo.fr/?editDatsId=745	Public after registration	doi:10.6096/MISTRALS-HyMeX.745	zip1
			EPFL-LTE Disdrometers (at least 6 instruments for Fall 2012 and Fall 2013)		http://mistrals.sedoo.fr/?editDatsId=899	Public after registration	doi:10.6096/MISTRALS-HyMeX.899	zip1
	Disdrometer (Parsivel 2)	Res	DSD network, Saint-Etienne-de-Fontbellon	[a]	http://mistrals.sedoo.fr/?editDatsId=744		doi:10.17178/OHMCV.DSD.SEF.12-14.1	zip1
			DSD network, Villeneuve-de-Berg-1	[a]	http://mistrals.sedoo.fr/?editDatsId=680	Public after registration	doi:10.17178/OHMCV.DSD.VB1.12-14.1	zip1
			DSD network, Villeneuve-de-Berg-2	[a]	http://mistrals.sedoo.fr/?editDatsId=681	Public after registration	doi:10.17178/OHMCV.DSD.VB2.11-14.1	zip1
			DSD network, Villeneuve-de-Berg-3	[a]	http://mistrals.sedoo.fr/?editDatsId=682	Public after registration	doi:10.17178/OHMCV.DSD.VB3.12-14.1	zip1
	Rain gauge (SPC Grand Delta)	Op	SPCGD French rain gauges (Berzème, Escrinet, Pont d'Ucel, Vogüe)	[a]	http://mistrals.sedoo.fr/?editDatsId=1444	Public after registration	no	zip1
	Rain gauge (Hpiconet)	Res	Hpiconet rain gauge network	[a]	http://mistrals.sedoo.fr/?editDatsId=656	Public after registration	doi:10.17178/OHMCV.RTS.AUZ.10-14.1	zip1
	Rainfall reanalysis	Res	Pluviometric reanalysis Cévennes-Vivarais		http://mistrals.sedoo.fr/?editDatsId=1183	Public after registration	doi:10.17178/OHMCV.REA.CEV.07-14.1	zip1
Meteorology	Baro-Diver	Res	Limnimeter network, Gazel and Claduègne catchments		http://mistrals.sedoo.fr/?editDatsId=994	Public after registration	doi:10.17178/OHMCV.LIM.CLA.12-14.1	zip1
Surface water	Hydrometric stations	Res	Gazel and Claduègne hydro-sedimentary stations	[a]	http://mistrals.sedoo.fr/?editDatsId=993	Public after registration	doi:10.17178/OHMCV.HSS.CLA.11-14.1	zip1
			Acoustic Doppler Velocimeter IQ Plus, Claduègne		http://mistrals.sedoo.fr/?editDatsId=1349	Public after registration	doi:10.17178/OHMCV.ADV.CLA.13-14.1	zip1
			LSPIV gauging stations (Auzon hydrometric station)	[a]	http://mistrals.sedoo.fr/?editDatsId=996	Public after registration	doi:10.17180/OBS.OHM-CV.ARDECHE	zip1
	Water erosion plots	Res	Runoff and erosion plots, Pradel		http://mistrals.sedoo.fr/?editDatsId=1347	Public after registration	doi:10.17178/OHMCV.ERO.PRA.10-13.1	zip1
	Stream sensors network	Res	Llimnimeter network, Gazel and Claduègne catchments		http://mistrals.sedoo.fr/?editDatsId=994	Public after registration	doi:10.17178/OHMCV.LIM.CLA.12-14.1	zip1
Soil	ThetaProbe	Res	Soil Moisture Gazel		http://mistrals.sedoo.fr/?editDatsId=1179	Public after registration	doi:10.6096/MISTRALS-HyMeX.1179	zip1
	10 HS	Res	Soil moisture sensor network, Gazel and Claduègne catchments		http://mistrals.sedoo.fr/?editDatsId=1350	Public after registration	doi:10.17178/OHMCV.SMO.CLA.13-14.1	zip1

[a] Means that the instrument(s) is (are) still running at the date of publication of the paper and at least for the period of LOP (long-term observation period, 2010–2020) of the HyMeX program.
[b] A simple registration (name, affiliation, e-mail) is necessary to create an account (http://mistrals.sedoo.fr/User-Account-Creation/). An e-mail with login and password is instantaneously sent which enables direct access to public data.
[c] To facilitate the use of the data and avoid downloading each individual datasets, a bundling service was provided: the "zip1" file (with the same structure as Table 5). The bundled data present the advantage of gathering data in ASCII and Cartesian format, in a single coordinate system and in the same time zone (UTC). The bundled data are selected for the spatial and temporal windows presented in the paper since some individual datasets have different extents. The "zip1" file (602 MB) is accessible directly (without registration) by clicking on the purple icon of the "data access" section of the page http://mistrals.sedoo.fr/MISTRALS/?editDatsId=1438.

Table 6. Overview of the URL links and DOIs that allow access to the public GIS descriptors presented in this study.

GIS descriptor	Data	Dataset name	Data access	Status within Mistrals/HyMeX database[b]	DOI	Included in bundled data[c]
Topography	1 m bare-earth DTM of Cladugne catchment	Digital Terrain Model (DTM) Lidar of Cladugne catchment	http://mistrals.sedoo.fr/?editDatsId=1178	Public after registration	10.6096/MISTRALS-HyMeX.1178	zip1
	5 m bare-earth DTM of Auzon catchment	Digital Terrain Model (DTM) of the Auzon catchment region	http://mistrals.sedoo.fr/?editDatsId=1389	Public after registration	10.6096/MISTRALS-HyMeX.1389	zip1
Soil properties	Soil depth for each SCU[a]	Soil properties Auzon catchment	http://mistrals.sedoo.fr/?editDatsId=1385	Public after registration	10.6096/MISTRALS-HyMeX.1385	zip1
	Maximum soil water storage for each SCU	Soil properties Auzon catchment	http://mistrals.sedoo.fr/?editDatsId=1385	Public after registration	10.6096/MISTRALS-HyMeX.1385	zip1
	Soil texture of superficial layer for each SCU	Soil properties Auzon catchment	http://mistrals.sedoo.fr/?editDatsId=1385	Public after registration	10.6096/MISTRALS-HyMeX.1385	zip1
	Soil stone content for each SCU	Soil properties Auzon catchment	http://mistrals.sedoo.fr/?editDatsId=1385	Public after registration	10.6096/MISTRALS-HyMeX.1385	zip1
Infiltration tests	Infiltration campaign Cladugne catchment	Infiltration campaign Cladugne catchment, Ardèche, France	http://mistrals.sedoo.fr/?editDatsId=1321	Public after registration	10.6096/MISTRALS-HyMeX.1321	zip1
Land use	5 m resolution images of Cladugne catchment	Landcover map Cladugne catchment	http://mistrals.sedoo.fr/?editDatsId=1381	Public after registration	10.14768/MISTRALS-HYMEX.1381	zip1
	30 m resolution images of Auzon catchment	Landcover map Ardeche, Cèze and Gardon Bassins	http://mistrals.sedoo.fr/?editDatsId=1377	Public after registration	10.14768/MISTRALS-HYMEX.1377	zip1
Surface information	Catchment boundaries	Surface information Auzon catchment	http://mistrals.sedoo.fr/?editDatsId=1390	Public after registration	10.6096/MISTRALS-HyMeX.1390	zip1
	Drainage network (stream)	Surface information Auzon catchment	http://mistrals.sedoo.fr/?editDatsId=1390	Public after registration	10.6096/MISTRALS-HyMeX.1390	zip1
	Instruments	Surface information Auzon catchment	http://mistrals.sedoo.fr/?editDatsId=1390	Public after registration	10.6096/MISTRALS-HyMeX.1390	zip1

[a] SCU: soil cartographic unit.
[b] A simple registration (name, affiliation, e-mail) is necessary to create an account (http://mistrals.sedoo.fr/User-Account-Creation/). An e-mail with login and password is instantaneously sent which enables direct access to public data.
[c] To facilitate the use of the data and avoid downloading each individual datasets, a bundling service was provided: the "zip1" file (with the same structure as Table 6). The bundled data have the advantage of gathering data in ASCII and Cartesian format in a single coordinate system and in the same time zone (UTC). The bundled data are selected for the spatial and temporal windows presented in the paper since some individual datasets have different extents. The "zip1" file (602 MB) is accessible directly (without registration) clicking on the purple icon of the "data access" section of the page http://mistrals.sedoo.fr/MISTRALS/?editDatsId=1438.

Table 7. Overview of the URL links and DOI that allow access to the additional datasets presented in this study. The datasets are organized by instrument.

Compartment	Instrumental device/ instrument	Op/Res	Dataset name		Mistrals data access	Status within Mistrals/HyMeX database[b]	DOI	Included in bundled data[c]
Rainfall	S-band Doppler and polarimetric radar	Op	Operational Weather Radar ARAMIS, BOLLENE, 5 min reflectivity and radial wind speed	[a]	http://mistrals.sedoo.fr/?editDatsId=705	Associated scientists	No	No
			Operational Weather Radar ARAMIS, BOLLENE, 5 min cumulative rainfall in mm	[a]	http://mistrals.sedoo.fr/?editDatsId=695	Associated scientists	No	No
			Operational Weather Radar ARAMIS, NIMES, 5 min reflectivity and radial wind speed	[a]	http://mistrals.sedoo.fr/?editDatsId=708	Associated scientists	No	No
			Operational Weather Radar ARAMIS, NIMES, 5 min cumulative rainfall in mm	[a]	http://mistrals.sedoo.fr/?editDatsId=699	Associated scientists	No	No
			French Radar composite 5 min cumulative rainfall in mm	[a]	http://mistrals.sedoo.fr/?editDatsId=703	Associated scientists	No	No
	Micro Rain Radar MRR-2	Res	Micro Rain Radar CNRM Le Pradel		http://mistrals.sedoo.fr/?editDatsId=1110	Associated scientists	No	No
	Rain gauge Météo-France	Op	Operational surface weather observation stations over France – hourly data	[a]	http://mistrals.sedoo.fr/?editDatsId=627	Associated scientists	No	zip2
Meteorology	Weather stations	Op	Operational surface weather observation stations over France – hourly data	[a]	http://mistrals.sedoo.fr/?editDatsId=627	Associated scientists	No	zip2
Soil	ThetaProbe ML2X	Op	SMOSMANIA – Soil moisture and temperature, France		http://mistrals.sedoo.fr/?editDatsId=469	Associated scientists	No	zip2

[a] The instrument(s) is (are) still running at the date of publication of the paper and at least for the period of LOP (long-term observation period, 2010–2020) of the HyMeX programme.

[b] The validation of the HyMeX data policy (http://mistrals.sedoo.fr/HyMeX/Data-Policy/HyMeX_DataPolicy.pdf) is necessary to access datasets under "associated scientists" status. There are two options. (1) The user had registered previously for access to public data only. In this case, he/she must go to his/her account (http://mistrals.sedoo.fr/Your-Account/) and complete the HyMeX registration application. (2) The user registers for the first time. He/she must go to http://mistrals.sedoo.fr/User-Account-Creation/, not checking the box corresponding to "Simple registration (name, affiliation, country) for direct access to public data only", and follow the registration.

[c] To facilitate the use of the data and avoid downloading each individual dataset, a bundling service was provided: the "zip2" file (with the same structure as Table 7). The bundled data have the advantage of gathering data in ASCII and Cartesian format in a single coordinate system and in the same time zone (UTC). The bundled data are selected for the spatial and temporal windows presented in the paper since some individual datasets have different extents. The "zip2" file (4 MB) is accessible clicking on the blue icon of the "data access" section of the page http://mistrals.sedoo.fr/MISTRALS/?editDatsId=1438.

2007–2014 period (Boudevillain et al., 2016) based on the merging of operational radar and rain gauge data has been added to Table 5 as it represents a useful dataset for many hydrological studies. All the individual datasets listed in Tables 5, 6, and 7 have a specific metadata record (see URL links in corresponding tables) in the HyMeX Database (http://mistrals.sedoo.fr/HyMeX/) maintained by the ESPRI/IPSL and SEDOO/Observatoire Midi-Pyrénées in France. The metadata record includes many fields, amongst which the dataset name, the period of observation, the principal investigator in charge of the dataset, a description of the data, the geographic coordinates of the instruments, a description of the instruments and the measured variables, the format of the data and the status of the data. The metadata record also has a "data access" section. For the public datasets (Tables 5 and 6), a simple registration (name, affiliation, e-mail) is necessary to create an account (http://mistrals.sedoo.fr/User-Account-Creation/). This simple registration generates an automatic e-mail with login and password which enables direct access to public data. For the additional datasets under "associated scientists" status (Table 7), the validation of the HyMeX data policy (http://mistrals.sedoo.fr/HyMeX/Data-Policy/HyMeX_DataPolicy.pdf) is necessary to access the data. There are two options.

1. (1) The user had registered previously for access to public data only. In this case, he/she must go to his/her account (http://mistrals.sedoo.fr/Your-Account/) and complete the HyMeX registration application.

2. (2) The user registers for the first time. He/she must go to http://mistrals.sedoo.fr/User-Account-Creation/, not checking the box corresponding to "Simple registration (name, affiliation, country) for direct access to public data only", and follow the registration.

Additionally a bundling service was performed to facilitate the use of the data. The bundled data include the most commonly used data in hydrometeorological and hydrological studies. The bundled data have the advantage of gathering data in ASCII and Cartesian format in a single coordinate system and in the same time zone (UTC). The bundled data are selected for the spatial and temporal windows presented in the paper (see the extent of Figs. 3 and 6) since some individual datasets have different extents. For the remaining datasets, not included in the bundled data, the effort to prepare the data was judged too laborious and their potential more restricted. Such datasets remain accessible individually even though they are not necessarily in the same format and with the same extent (polar vs. Cartesian and coordinate system). The bundled data are organized in two independent ways: (i) for the public datasets which refer to Tables 5 and 6, the "zip1" file (602 MB) is accessible directly (without registration) clicking on the purple icon of the "data access" section of the page http://mistrals.sedoo.fr/MISTRALS/?editDatsId=1438; (ii) for the additional datasets subject to the HyMeX data policy, the "zip2" file (4 MB) is accessible by clicking on the blue icon of the "data access" section of the page http://mistrals.sedoo.fr/MISTRALS/?editDatsId=1438.

Alternatively, there are other ways to access and visualize the data: the SEVnOL system, maintained by IGE, on the OHMCV website (http://www.ohmcv.fr) and the BDOH database (https://bdoh.irstea.fr/OHM-CV/) maintained by IRSTEA and managed by the data producers (IRSTEA, IGE). SEVnOL and BDOH are complementary tools to the bundling service proposed in this study (through the release of the "zip1" and "zip2" files). BDOH was developed for the management of long-term time series and enables the following features: visualization of data, downloading of data, interpolation of time steps for export, import and export to multiple formats, and automatic calculation of derived time series. SEVnOL is a web interface developed to view and extract data, metadata and products in several formats (XML, CSV, NetCDF) over a user-defined spatial and temporal window (Boudevillain et al., 2011).

6 Conclusion

A high space–time resolution dataset linking hydrometeorological forcing and hydro-sedimentary response in a mesoscale catchment is presented. The Auzon catchment (116 km^2), a tributary of the Ardèche River, is subject to precipitating systems of Mediterranean origin, which can result in significant rainfall amount. The data presented cover a period of 4 years (2011–2014), including the HyMeX-SOP1 field campaign (Ducrocq et al., 2014) and the ANR Flood-Scale project (Braud et al., 2014), which aims at improving the understanding of processes triggering flash floods. The multi-scale observation system presented is part of the OHMCV (Boudevillain et al., 2011). The operational and research networks provide high space–time resolution data (< 1 km^2, 5 min) for studying the microphysics of precipitating systems and producing QPE particularly adapted to fine-scale hydrological studies. The measurement of the other meteorological variables relies almost exclusively on the operational network (1 h time resolution). Validation data are both spatially distributed and multi-scale. They include point measurements of soil moisture (fixed sensors in continuous mode and mobile sensors during rain events), runoff and erosion measurements on hillslope, water level measurements in the intermittent hydrographic network of headwater catchments (11 points of measurement) and hydrometric measurements (discharge, water conductivity and temperature) at the outlet of three nested catchments (3.4, 44 and 116 km^2). Discharge measurements were made at high water levels during on-alert campaigns to establish stage–discharge relationships. It is hoped that using this dataset will lead to advances in understanding hydrological processes leading to flash floods and improving distributed hydrological models.

Appendix A

Table A1. Abbreviations used in this article.

CNRM	Centre National de Recherches Météorologiques, National Centre for Meteorological Research
EPFL	École Polytechnique Fédérale de Lausanne, Swiss Federal Institute of Technology
ESPRI/IPSL	Ensemble de Services Pour la Recherche de l'Institut Pierre Simon Laplace, Research oriented services of the Pierre Simon Laplace Institute
IGE	Institut des Géosciences de l'Environnement, Institute of Environmental Geosciences
IRSTEA	Institut national de Recherche en Sciences et Technologies pour l'Environnement et l'Agriculture, National Research Institute of Science and Technology for Environment and Agriculture
LaMP	Laboratoire de Météorologie Physique, Laboratory of Physical Meteorology
OSUG	Observatoire des Sciences de l'Univers de Grenoble, Observatory of Sciences of the Universe of Grenoble
SEDOO	Service de DOnnées de l'Observatoire Midi-Pyrénées, Data management service of the Midi-Pyrénées Observatory

Table A2. Summary of the period of operation of the instruments. The number of instruments in operation is also indicated given that many instruments belong to a network of sensors. Op/Res column indicates whether the instruments belong to an operational observation network ("Op") or a research observation network ("Res").

Compartment	Instrumental device	Op/Res	Instrument		2011																								2012																							
					1		2		3		4		5		6		7		8		9		10		11		12		1		2		3		4		5		6		7		8		9		10		11		12	
Rainfall		Op	S-band Doppler and polarimetric radar	*	2	2	2	2	2	2	2	2	2	2	2	2	2	2	2	2	2	2	2	2	2	2	2	2	2	2	2	2	2	2	2	2	2	2	2	2	2	2	2	2	2	2	2	2	2	2	2	2
		Res	X-band Doppler and polarimetric radar (MXPol)																																												1	1	1	1		
		Res	X-band fast-scanning radar (WR-10X+11)																																												1	1				
		Res	Micro Rain Radar (MRR-2)																																											2	2	2	2		
		Res	Disdrometer (Parsivel 1)		1	1	1	1	1	1	1	1	1	1	1	1	1	1	1	1	1	1	1	1	1	2	2	2	2	2	2	2	2	2	2	2	2	2	2	2	2	2	9	9	9	8	8	8	1	1
		Res	Disdrometer (Parsivel 2)																							3	3	3	3	3	3	3	3	3	3	3	3	3	3	3	3	3	4	4	4	4	4	4	4	4	4
		Op	Rain gauge (Météo-France, SPC Grand Delta)		10	10	10	10	10	10	10	10	10	10	10	10	10	10	10	10	10	10	10	10	10	10	10	10	10	10	10	10	10	10	10	10	10	10	10	10	10	10	10	10	10	10	10	10	10	10
		Res	Rain gauge (Hpiconet)	*	5	5	5	6	6	6	6	6	6	6	6	6	6	6	6	6	6	6	6	6	9	9	17	17	17	17	17	18	18	17	17	18	18	15	15	15	13	8	8	8	18	15	15	16	12	12	15	14
Meteorology		Op	Temperature probe (PT100)	*																	6	6	6	6	6	6	6	6																	6	6	6	6	6	6	6	6
		Res	Baro-Diver (DI500, Mini-Diver DI501)																																										1	1	1	1	1	1	2	2
		Op	Humidity probe (HMP45D)	*																	6	6	6	6	6	6	6	6																	6	6	6	6	6	6	6	6
		Op	Barometer (PTB220)	*																	1	1	1	1	1	1	1	1	1	1	1	1	1	1	1	1	1	1	1	1	1	1	1	1	1	1	1	1	1	1	1	1
		Op	Wind sensor (DEOLIA 96, Alizia 312)	*																	3	3	3	3	3	3	3	3	3	3	3	3	3	3	3	3	3	3	3	3	3	3	3	3	3	3	3	3	3	3	3	3
		Op	Pyranometer (Kipp & Zonen)	*																	2	2	2	2	2	2	2	2	2	2	2	2	2	2	2	2	2	2	2	2	2	2	2	2	2	2	2	2	2	2	2	2
Surface water	Hydrometric stations	Res	Pressure probe (PLS)	*								1	1	1	1	1	1	1	1	1	1	1	1	1	1	1	1	1	1	1	1	1	1	1	1	1	1	1	1	1	1	1	1	1	1	1	1	1	1	1	1
		Res	Radar level sensor (Cruzoe)	*																1	1	1	1	1	1	1	1	1	1	1	1	1	1	1	1	1	1	1	1	1	1	1	1	1	1	1	1	1	1	1	1
		Res	Radar level sensor (RLS)	*																																																
		Res	LSPIV/camera (VW-BP330)	*																																																
		Res	Radar surface velocity sensor (RG-30)	*																																											1	1	1	1	1	1	1	1
		Res	Acoustic Doppler velocimeter (IQ Plus)																																																	
		Res	Conductivity and temp. probe (CS547)	*									1	1	1	1	1	1	1	1	1	1	2	2	2	2	2	2	2	2	2	2	2	2	2	2	2	2	2	2	2	2	2	2	2	2	2	2	2	2	2	2
		Res	Suspended solids probe (Visolid IQ 700)	*									1	1	1	1	1	1	1	1	1	1	2	2	2	2	2	2	2	2	2	2	2	2	2	2	2	2	2	2	2	2	2	2	2	2	2	2	2	2	2	2
		Res	3700 portable sampler	*									1	1	1	1	1	1	1	1	1	1	2	2	2	2	2	2	2	2	2	2	2	2	2	2	2	2	2	2	2	2	2	2	2	2	2	2	2	2	2	2
	Water erosion plots	Res	HS flume with level sensor (Thalimedes)		2	2	2	2	2	2	2	2	2	2	2	2	2	2	2	2	2	2	2	2	2	2	2	2	2	2	2	2	2	2	2	2	2	2	2	2	2	2	2	2	2	2	2	2	2	2	2	2
		Res	3700 portable sampler		2	2	2	2	2	2	2	2	2	2	2	2	2	2	2	2	2	2	2	2	2	2	2	2	2	2	2	2	2	2	2	2	2	2	2	2	2	2	2	2	2	2	2	2	2	2	2	2
	Limnimeter network	Res	Mini-Diver (DI501)																																																	
		Res	CTD-Diver (DI271)																																																	
Soil	Soil moisture network	Res	ThetaProbe																																																	
		Res	10 HS																																																	
		Res	ThetaProbe (ML2X)		1	1	1	1	1	1	1	1	1	1	1	1	1	1	1	1	1	1	1	1	1	1	1	1	1	1	1	1	1	1	1	1	1	1	1	1	1	1	1	1	1	1	1	1	1	1	1	1

Compartment	Instrumental device	Op/Res	Instrument		2013																								2014																							
					1		2		3		4		5		6		7		8		9		10		11		12		1		2		3		4		5		6		7		8		9		10		11		12	
Rainfall		Op	S-band Doppler and polarimetric radar	*	2	2	2	2	2	2	2	2	2	2	2	2	2	2	2	2	2	2	2	2	2	2	2	2	2	2	2	2	2	2	2	2	2	2	2	2	2	2	2	2	2	2	2	2	2	2	2	2
		Res	X-band Doppler and polarimetric radar (MXPol)																	1	1	1	1	1																													
		Res	X-band fast-scanning radar (WR-10X+11)																																																	
		Res	Micro Rain Radar (MRR-2)																	1	3	3	3	3	3	3	1																											
		Res	Disdrometer (Parsivel 1)		1	1	1	1	1	1	1	1	1	1	1	1	1	2	2	3	8	9	11	11	11	8	2	2	2	2	2	2	2	1	1	2	2	2	2	2	2	10	7	9	8	8	10	8	8
		Res	Disdrometer (Parsivel 2)		4	4	4	4	4	4	4	4	4	4	4	4	4	4	4	3	4	4	4	4	4	3	3	3	3	3	3	3	4	4	4	4	4	4	4	4	4	4	4	4	3	4	4	4	4	4	4	4
		Op	Rain gauge (Météo-France, SPC Grand Delta)		10	10	10	10	10	10	10	10	10	10	10	10	10	10	10	10	10	10	10	10	10	10	10	10	10	10	10	10	10	10	10	10	10	10	10	10	10	10	10	10	10	10	10	10	10	10	10	10
		Res	Rain gauge (Hpiconet)	*	14	14	13	14	17	16	16	18	18	18	18	18	17	16	17	17	18	18	20	19	18	20	20	19	19	19	20	20	20	20	18	18	18	18	18	18	18	18	19	19	20	20	0	0	0	0
Meteorology		Op	Temperature probe (PT100)	*	6	6	6	6	6	6											6	6	6	6	6	6	6	6																	6	6	6	6	6	6	6	6
		Res	Baro-Diver (DI500), Mini-Diver (DI501)		2	2	2	2	3	3	4	4	4	4	4	4	4	4	4	4	4	4	4	4	4	4	4	4	4	4	4	4	4	4	4	4	4	4	4	4	4	4	4	4	4	4	4	4	4	4	4	4
		Op	Humidity probe (HMP45D)	*	6	6	6	6	6	6											6	6	6	6	6	6	6	6																	6	6	6	6	6	6	6	6
		Op	Barometer (PTB220)	*	1	1	1	1	1	1											1	1	1	1	1	1	1	1																	1	1	1	1	1	1	1	1
		Op	Wind sensor (DEOLIA 96, Alizia 312)	*	3	3	3	3	3	3											3	3	3	3	3	3	3	3																	3	3	3	3	3	3	3	3
		Op	Pyranometer (Kipp & Zonen)	*	2	2	2	2	2	2											2	2	2	2	2	2	2	2																	2	2	2	2	2	2	2	2
Surface water	Hydrometric stations	Res	Pressure probe (PLS)	*	1	1	1	1	1	1	1	1	1	1	1	1	1	1	1	1	1	1	1	1	1	1	1	1	1	1	1	1	1	1	1	1	1	1	1	1	1	1	1	1	1	1	1	1	1	1	1	1
		Res	Radar level sensor (Cruzoe)	*	1	1	1	1	1	1	1	1	1	1	1	1	1	1	1	1	1	1	1	1	1	1	1	1	1	1	1	1	1	1	1	1	1	1	1	1	1	1	1	1	1	1	1	1	1	1	1	1
		Res	Radar level sensor (RLS)	*													1	1	1	1	1	1	1	1	1	1	1	1	1	1	1	1	1	1	1	1	1	1	1	1	1	1	1	1	1	1	1	1	1	1	1	1
		Res	LSPIV/analogical camera (VW-BP330)	*													1	1	1	1	1	1	1	1	1	1	1	1	1	1	1	1	1	1	1	1	1	1	1	1	1	1	1	1	1	1	1	1	1	1	1	1
		Res	Radar surface velocity sensor (RG-30)	*	1	1	1	1	1	1	1	1	1	1	1	1	1	1	1	1	1	1	1	1	1	1	1	1	1	1	1	1	1	1	1	1	1	1	1	1	1	1	1	1	1	1	1	1	1	1	1	1
		Res	Acoustic Doppler velocimeter (IQ Plus)														1	1	1	1	1	1	1	1	1	1	1	1	1	1	1	1	1	1	1	1	1	1	1	1	1	1	1	1	1	1	1	1	1	1	1	1
		Res	Conductivity and temp. probe (CS547)	*	2	2	2	2	2	2	2	2	2	2	2	2	2	2	2	2	2	2	2	2	2	2	2	2	2	2	2	2	2	2	2	2	2	2	2	2	2	2	2	2	2	2	2	2	2	2	2	2
		Res	Suspended solids probe Visolid (IQ 700)	*	2	2	2	2	2	2	2	2	2	2	2	2	2	2	2	2	2	2	2	2	2	2	2	2	2	2	2	2	2	2	2	2	2	2	2	2	2	2	2	2	2	2	2	2	2	2	2	2
		Res	3700 portable sampler	*	2	2	2	2	2	2	2	2	2	2	2	2	2	2	2	2	2	2	2	2	2	2	2	2	2	2	2	2	2	2	2	2	2	2	2	2	2	2	2	2	2	2	2	2	2	2	2	2
	Water erosion plots	Res	HS flume with level sensor (Thalimedes)		2	2	2	2	2	2	2	2	2	2	2	2	2	2	2	2	2	2	2	2	2	2	2																									
		Res	3700 portable sampler		2	2	2	2	2	2	2	2	2	2	2	2	2	2	2	2	2	2	2	2	2	2	2																									
	Limnimeter network	Res	Mini-Diver (DI501)		3	3	3	3	3	3	3	3	3	3	3	3	3	3	3	3	3	3	3	3	3	3	3	3	3	3	3	4	4	4	4	4	3	3	3	3	3	3	3	3	3	3	3	3	3	3	3	3
		Res	CTD-Diver (DI271)		5	5	5	5	5	5	5	5	5	5	5	5	5	5	5	5	5	5	5	5	5	5	5	5	5	5	5	5	5	5	5	5	5	5	5	4	6	6	6	6	6	6	6	6	6	6	6	6
Soil	Soil moisture network	Res	ThetaProbe																																																
		Res	10 HS												9	9	9	9	9	9	9	9	9	9	9	9	9		9	9	9	9	9	9	9	9	9	9	9	9	9	9	9	9	9	9	9	9	9			
		Res	ThetaProbe (ML2X)		1	1	1	1	1	1	1	1	1	1	1	1	1	1	1	1	1	1	1	1	1	1	1	1	1	1	1	1	1	1	1	1	1	1	1	1	1	1	1	1	1	1	1	1	1	1	1	1

* The instrument(s) is (are) still running at the date of publication of the paper and at least for the LOP (long-term observation period, 2010–2020) of the HyMeX programme.
For each year from 2011 to 2014, the number of operating instruments is indicated by fortnightly period (the months are numbered from 1 to 12).
Fields with numbers indicates the periods when instruments operate, whereas blank fields indicate periods without any measurements.

Appendix B

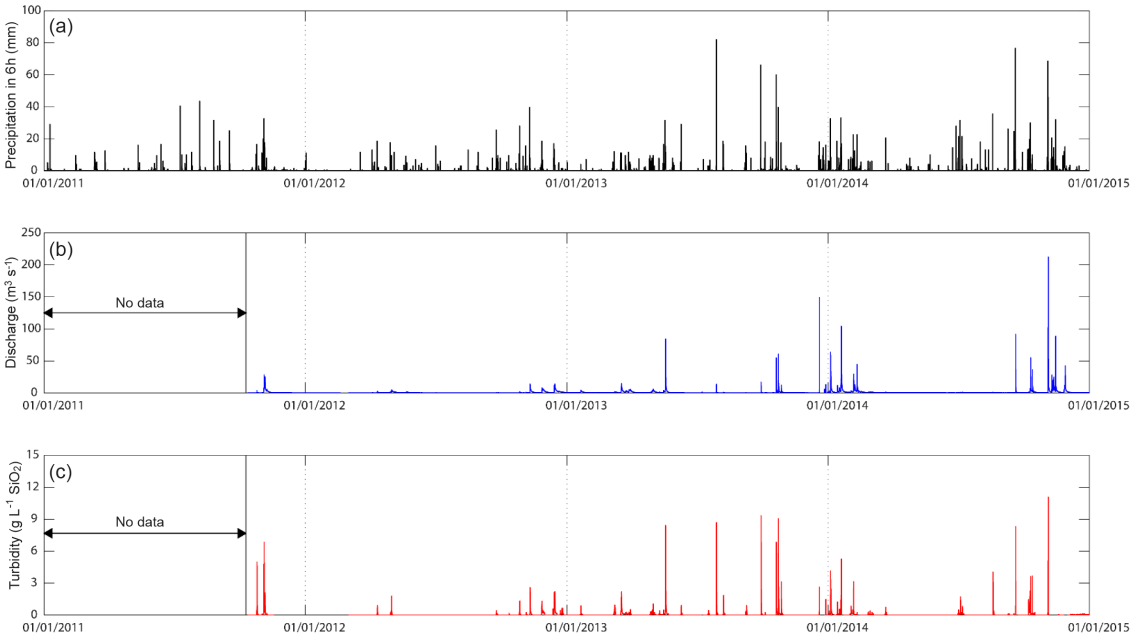

Figure B1. Overview of the **(a)** 6 h accumulated rainfall, **(b)** discharge (10 min time step) and **(c)** turbidity (10 min time step) for the entire record (period 2011–2014) at the Claduègne hydrometric station. The rainfall data presented were taken from the operational Météo-France rain gauge "Mirabel-SA" displayed in Fig. 3. Note the 4 November 2014 flood is a 5–10-year return period flood for the Claduègne River.

Author contributions. Guillaume Nord, Brice Boudevillain, Alexis Berne, Guillaume Dramais, Cédric Legoût, Gilles Molinié, Joel Van Baelen, and Jean-Pierre Vandervaere were principal investigators responsible for specific instruments or networks of instruments which resulted in the main individual datasets presented in this study. Isabelle Braud was the leader of the FloodScale (2012–2015) ANR project. Flora Branger, Isabelle Braud, Jérôme Le Coz, Guy Delrieu, Guillaume Nord, and Jean-Pierre Vandervaere were responsible for work packages within the FloodScale project which contributed significantly to the design of the observation system presented in this study. Simon Gérard, Martin Calianno, and Coralie Aubert helped in installing and maintaining the observation system. Julien Andrieu prepared the land use maps. Guillaume Nord prepared the manuscript with contributions from all co-authors. Flora Branger and Ivan Horner helped with elaborating Figs. 7 and 8. Guillaume Nord, Brice Boudevillain, and Isabelle Braud managed the process of data preparation and DOI attribution to the individual datasets for subsequent submission to *Earth System Science Data*. Guillaume Nord and Brice Boudevillain contributed to the bundling of the data. Brice Boudevillain performed the selection of the individual datasets for the spatial and temporal windows presented in the paper. All co-authors contributed to the data collection or evaluation of the individual datasets presented in this study.

Competing interests. The authors declare that they have no conflict of interest.

Acknowledgements. The FloodScale project is funded by the French National Research Agency (ANR) under contract no. ANR 2011 BS56 027, which contributes to the HyMeX programme. It also benefits from funding by the MISTRALS/HyMeX programme (http://www.mistrals-home.org). OHMCV is supported by the Institut National des Sciences de l'Univers (INSU/CNRS), the French Ministry for Education and Research, the Environment Research Cluster of the Rhône-Alpes Region, the Observatoire des Sciences de l'Univers de Grenoble (OSUG) and the SOERE Réseau des Bassins Versants (Alliance Allenvi). The development of the BDOH database was supported by Irstea internal funding and the Rhône Sediment Observatory (OSR) project, partly funded by the Plan Rhône. The equipment of the erosion plots and part of the Gazel hydrometric station was funded by the Rhône-Alpes Region. The Sontek-IQ Plus instrument was funded by the French National Research Agency (ANR) under contract no. ANR-12-JS06-0006 (SCAF project). The authors thank the providers of operational data: Météo-France and the SPC Grand Delta. The contract of Simon Gérard was funded by the Institut National des Sciences de l'Univers (INSU/CNRS). The PhD thesis of Annette Wijbrans was funded by Rhône-Alpes Region. We warmly thank colleagues of IGE (especially Romain Biron who participated at the beginning of the project), including students and technical staff (with special thoughts to Matthieu Le Gall), who helped in installing and maintaining the observation system. We also thank Isabella Zin and Jérémy Chardon for providing the analogue rainfall forecasting. IGE is part of Labex OSUG@2020 (ANR10 LABX56), which funded the contract of Martin Calianno, who also assisted with the first installations. The HyMeX database teams (ESPRI/IPSL and SEDOO/Observatoire Midi-Pyrénées) and the team of the OSUG data centre helped in accessing the data and attributing DOIs to the individual datasets. In addition, the authors acknowledge the EPLEFPA Olivier de Serres; the municipalities of Lavilledieu, Lussas, Mirabel, Saint-Germain, Saint-Etienne de Fontbellon, and the middle school of Villeneuve de Berg; and the local landowners and neighbours for hosting the experiments. Timothy H. Raupach acknowledges the support from the Swiss National Science Foundation.

Edited by: K. Elger
Reviewed by: two anonymous referees

References

Baffaut, C., Ghidey, F., Sudduth, K. A., Lerch, R. N., and Sadler E. J.: Long-term suspended sediment transport in the Goodwater Creek Experimental Watershed and Salt River Basin, Missouri, USA, Water Resour. Res., 49, 7827–7830, doi:10.1002/wrcr.20511, 2013.

Berne, A. and Krajewski, W. F.: Radar for hydrology: Unfulfilled promise or unrecognized potential?, Adv. Water Resour., 51, 357–366, doi:10.1016/j.advwatres.2012.05.005, 2013.

Borga, M., Stoffel, M., Marchi, L., Marra, F., and Jakob, M.: Hydrogeomorphic response to extreme rainfall in headwater systems: Flash floods and debris flows, J. Hydrol., 518, 194–205, doi:10.1016/j.jhydrol.2014.05.022, 2014.

Bornand, M., Legros, J., and Moinereau, J.: Notice explicative de la carte pédologique de France à 1/100 000, Privas, INRA, Service d'étude des sols et de la carte pédologique de France, 255 pp., 1977.

Boudevillain, B., Delrieu, G., Galabertier, B., Bonnifait, L., Bouilloud, L., Kirstetter, P.-E., and Mosini, M.-L.: The Cévennes-Vivarais Mediterranean Hydrometeorological Observatory database, Water Resour. Res., 47, W07701, doi:10.1029/2010WR010353, 2011.

Boudevillain, B., Delrieu, G., Wijbrans, A., and Confoland, A.: A high-resolution rainfall re-analysis based on radar-raingauge merging in the Cévennes-Vivarais region, France, J. Hydrol., 541, 14–23, doi:10.1016/j.jhydrol.2016.03.058, 2016.

Bousquet, O., Berne, A., Delanoe, J., Dufournet, Y., Gourley, J. J., Van-Baelen, J., Augros, C., Besson, L., Boudevillain, B., Caumont, O., Defer, E., Grazioli, J., Jorgensen, D. J., Kirstetter, P.-E., Ribaud, J.-F., Beck, J., Delrieu, G., Ducrocq, V., Scipion, D., Schwarzenboeck, A., and Zwiebel, J.: Multifrequency Radar Observations Collected in Southern France during HyMeX-SOP1, B. Am. Meteorol. Soc., 96, 267–282, doi:10.1175/BAMS-D-13-00076.1, 2015.

Branger, F., Dramais, G., Horner, I., Boursicaud, R. L., Coz, J. L., and Renard, B.: Improving the quantification of flash flood hydrographs and reducing their uncertainty using noncontact streamgauging methods, EGU General Assembly, Vienna, Austria, 12–17 April 2015, EGU2015-5768, 2015.

Braud, I., De Condappa, D., Soria, J., Haverkamp, R., Angulo-Jaramillo, R., Galle, S., and Vauclin, M.: Use of scaled forms of the infiltration equation for the estimation of unsaturated soil hydraulic properties (Beerkan method), Eur. J. Soil Sci., 56, 361–374, doi:10.1111/j.1365_2389.2004.00660.x, 2005.

Braud, I., Ayral, P.-A., Bouvier, C., Branger, F., Delrieu, G., Le Coz, J., Nord, G., Vandervaere, J.-P., Anquetin, S., Adamovic, M., Andrieu, J., Batiot, C., Boudevillain, B., Brunet, P., Carreau, J., Confoland, A., Didon-Lescot, J.-F., Domergue, J.-M., Douvinet, J., Dramais, G., Freydier, R., Gérard, S., Huza, J., Leblois, E., Le Bourgeois, O., Le Boursicaud, R., Marchand, P., Martin, P., Nottale, L., Patris, N., Renard, B., Seidel, J.-L., Taupin, J.-D., Vannier, O., Vincendon, B., and Wijbrans, A.: Multi-scale hydrometeorological observation and modelling for flash flood understanding, Hydrol. Earth Syst. Sci., 18, 3733–3761, doi:10.5194/hess-18-3733-2014, 2014.

Braud, I. and Vandervaere, J. P.: Analysis of infiltration tests performed in the Cladugne catchment in May–June 2012, contribution to WP3.4 "Documentation and mapping of soil hydraulic properties, soil geometry and vegetation cover of small catchments" of the FloodScale (2012–2015) ANR project, 66 pp., available at: http://mistrals.sedoo.fr/?editDatsId=1321, last access: 1 October 2015.

Cea, L., Legout, C., Grangeon, T., and Nord, G.: Impact of model simplifications on soil erosion predictions: application of the GLUE methodology to a distributed event-based model at the hillslope scale, Hydrol. Process., 30, 1096–1113, doi:10.1002/hyp.10697, 2016.

Delrieu, G., Wijbrans, A., Boudevillain, B., Faure, D., Bonnifait, L., and Kirstetter, P. E.:. Geostatistical radar-raingauge merging: a novel method for the quantification of rainfall estimation error, Adv. Water Res., 71, 110–124, 2014.

Demir, I., Conover, H., Krajewski, W. F., Seo, B.-C., Goska, R., He, Y., McEniry, M. F., Graves, S. J., and Petersen, W.: Data Enabled Field Experiment Planning, Management, and Research using Cyberinfrastructure, J. Hydrometeorol., 16, 1155–1170, doi:10.1175/JHM-D-14-0163.1, 2015.

de Vente, J., Poesen, J., Verstraeten, G., Govers, G., Vanmaercke, M., Van Rompaey, A., Arabkhedri, M., and Boix-Fayos, C.: Predicting soil erosion and sediment yield at regional scales: Where do we stand?, Earth-Sci. Rev., 127, 16–29, doi:10.1016/j.earscirev.2013.08.014, 2013.

Dramais, G., Le Coz, J., Le Boursicaud, R., Gallavardin, A., Benmamar, D., and Hauet, A: Suivi hydrométrique par mesure vidéo sur le bassin versant de l'Ardèche, Irstea, doi:10.17180/OBS.OHM-CV.ARDECHE, 2015.

Drobinski, P., Ducrocq, V., Alpert, P., Anagnostou, E., Béranger, K., Borga, M., Braud, I., Chanzy, A., Davolio, S., Delrieu, G., Estournel, C., Filali Boubrahmi, N., Font, J., Grubisic, V., Gualdi, S., Homar, V., Ivancan-Picek, B., Kottmeier, C., Kotroni, V., Lagouvardos, K., Lionello, P., Llasat, M. C., Ludwig, W., Lutoff, C., Mariotti, A., Richard, E., Romero, R., Rotunno, R., Roussot, O., Ruin, I., Somot, S., Taupier-Letage, I., Tintore, J., Uijlenhoet, R., and Wernli, H.: HyMeX, a 10-year multidisciplinary program on the Mediterranean water cycle, B. Am. Meteorol. Soc., 95, 1063–1082, doi:10.1175/BAMS-D-12-00242.1, 2014.

Ducrocq, V., Braud, I., Davolio, S., Ferretti, R., Flamant, C., Jansa, A., Kalthoff, N., Richard, E., Taupier-Letage, I., Ayral, P.-A., Belamari, S., Berne, A., Borga, M., Boudevillain, B., Bock, O., Boichard, J.-L., Bouin, M.-N., Bousquet, O., Bouvier, C., Chiggiato, J., Cimini, D., Corsmeier, U., Coppola, L., Cocquerez, P., Defer, E., Delanoë, J., Di Girolamo, P., Doerenbecher, A., Drobinski, P., Dufournet, Y., Fourrié, N., Gourley, J., Labatut, L., Lambert, D., Le Coz, J., Marzano, F., Molinié, G., Montani, A., Nord, G., Nuret, M., Ramage, K., Rison, B., Roussot, O., Said, F., Schwarzenboeck, A., Testor, P., Van-Baelen, J., Vincendon, B., Aran, M., and Tamayo, J.: HyMeX-SOP1, the field campaign dedicated to heavy precipitation and flash-flooding in the North-Western Mediterranean, B. Am. Meteorol. Soc., 95, 1083–1100, doi:10.1175/BAMS-D-12-00244.1, 2014.

Elmi, S., Busnardo, R., Clavel, B., Camus, G., Kieffer, G., Bérard, P., and Michaëly, B.: Notice explicative de la carte géologique de la France à 1/50000, Aubenas, Éditions du BRGM Service géologique national, 170 pp., 1996.

Fabry, F.: On the determination of scale ranges for precipitation fields, J. Geophys. Res., 101, 12819–12826, 1996.

Fraedrich, K. and Larnder, C.: Scaling regimes of composite rainfall time series, Tellus A, 45, 289–298, doi:10.1034/j.1600-0870.1993.t01-3-00004.x, 1993.

Gonzalez-Sosa, E., Braud, I., Dehotin, J., Lassabatère, L., Angulo-Jaramillo, R., Lagouy, M., Branger, F., Jacqueminet, C., Kermadi, S., and Michel, K.: Impact of land use on the hydraulic properties of the topsoil in a small French catchment, Hydrol. Process., 24, 2382–2399, 2010.

Goodrich, D. C., Lane, L. J., Shillito, R. M., Miller, S. N., Syed, K. H., and Woolhiser, D. A.: Linearity of basin response as a function of scale in a semiarid watershed, Water Resour. Res., 33, 2951–2965, doi:10.1029/97WR01422, 1997.

Grangeon, T. : Etude multi-échelle de la granulométrie des particules fines générées par érosion hydrique : apports pour la modélisation, PhD thesis, Université Joseph Fourier, France, 204 pp., 2012.

Grazioli, J., Tuia, D., and Berne, A.: Hydrometeor classification from polarimetric radar measurements: a clustering approach, Atmos. Meas. Tech., 8, 149–170, doi:10.5194/amt-8-149-2015, 2015.

Grillot, J. C.: Contribution à l'étude géologique et hydrogéologique du massif des Coirons (Partie Occidentale), PhD thesis, Applied geology, Université des Sciences et Techniques du Languedoc, France, 97 pp., 1971.

Gupta, V. K., Mantilla, R., Troutman, B. M., Dawdy, D., and Krajewski, W. F.: Generalizing a nonlinear geophysical flood theory to medium-sized river networks, Geophys. Res. Lett., 37, L11402, doi:10.1029/2009GL041540, 2010.

Horner, I.: Quantification des incertitudes hydrométriques et bilans hydrologiques sur le bassin versant de l'Yzeron (ouest lyonnais), MS thesis, AgroCampus Ouest, France, 52 pp., 2014.

Huza, J., Teuling, A. J., Braud, I., Grazioli, J., Melsen, L. A., Nord, G., Raupach, T. H., and Uijlenhoet, R.: Precipitation, soil moisture and runoff variability in a small river catchment (Ardèche, France) during HyMeX Special Observation Period 1, J. Hydrol., 516, 330–342, doi:10.1016/j.jhydrol.2014.01.041, 2014.

Jetten, V., Govers, G., and Hessel, R.: Erosion models: quality of spatial predictions, Hydrol. Process., 17, 887–900, doi:10.1002/hyp.1168, 2003.

Kormos, P. R., Marks, D., Williams, C. J., Marshall, H. P., Aishlin, P., Chandler, D. G., and McNamara, J. P.: Soil, snow, weather, and sub-surface storage data from a mountain catchment in the rain–snow transition zone, Earth Syst. Sci. Data, 6, 165–173, doi:10.5194/essd-6-165-2014, 2014.

Krajewski, W. F., Ciach, G. J., and Habib, E.: An analysis of small-scale rainfall variability in different climatic regimes, Hydrolog. Sci. J., 48, 151–162, doi:10.1623/hysj.48.2.151.44694, 2003.

Le Coz, J., Hauet, A., Pierrefeu, G., Dramais, G., and Camenen, B.: Performance of image-based velocimetry (LSPIV) applied to flash-flood discharge measurements in Mediterranean rivers, J. Hydrol., 394, 42–52, 2010.

Le Coz, J., Renard, B., Bonnifait, L., Branger, F., and Le Boursicaud, R.: Combining hydraulic knowledge and uncertain gaugings in the estimation of hydrometric rating curves: A Bayesian approach, J. Hydrol., 509, 573–587, doi:10.1016/j.jhydrol.2013.11.016, 2014.

Levesque, V. A. and Oberg, K. A.: Computing discharge using the index velocity method, U.S. Geological Survey, Techniques and Methods 3-A23, 148 pp., 2012.

Marchi, L., Borga, M., Preciso, E., and Gaume, E.: Characterisation of selected extreme flash floods in Europe and implications for flood risk management, J. Hydrol., 394, 118–133, doi:10.1016/j.jhydrol.2010.07.017, 2010.

Marra, F., Nikolopoulos, E. I., Creutin, J. D., and Borga, M.: Radar rainfall estimation for the identification of debris-flow occurrence thresholds, J. Hydrol., 519, 1607–1619, 2014.

Mishra, K. V., Krajewski, W. F., Goska, R., Ceynar, D., Seo, B.-C., Kruger, A., Niemeier, J., Galvez, M. B., Thurai, M., Bringi, V. N., Tolstoy, L., Kucera, P., Petersen, W., Grazioli, J., and Pazmany, A.: Deployment and performance analyses of high-resolution iowa XPOL radar system during the NASA IFloodS campaign, J. Hydrometeorol., 17, 455–479, doi:10.1175/JHM-D-15-0029.1, 2016.

Molinié, G., Ceresetti, D., Anquetin, S., Creutin, J. D., and Boudevillain, B.: Rainfall Regime of a Mountainous Mediterranean Region: Statistical Analysis at Short Time Steps, J. Appl. Meteorol. Clim., 51, 429–448, 2012.

National Advisory Committee for Aeronautics: Manual of the ICAO Standard Atmosphere Calculations by the NACA, Technical Note 3182, Washington, available at: http://ntrs.nasa.gov/archive/nasa/casi.ntrs.nasa.gov/19930083952.pdf, last access: 10 June 2015, 1954.

Naud, G.: Contribution à l'étude géologique et hydrogéologique du massif des Coirons (Partie Orientale), PhD thesis, Université de Provence, France, 153 pp., 1972.

Navratil, O., Esteves, M., Legout, C., Gratiot, N., Némery, J., Willmore, S., and Grangeon, T.: Global uncertainty analysis of suspended sediment monitoring using turbidimeter in a small mountainous river catchment, J. Hydrol., 398, 246–259, 2011.

Navratil, O., Evrard, O., Esteves, M., Legout, C., Ayrault, S., Nemery, J., Mate-Marin, A., Ahmadi, M., Lefevre, I., Poirel, A., and Bonte, P.: Temporal variability of suspended sediment sources in an alpine catchment combining river/rainfall monitoring and sediment fingerprinting, Earth Surf. Proc. Land., 37, 828–846, 2012.

Nicolas, M.: Etude expérimentale et numérique du ruissellement de surface: effets des variations d'intensité de la pluie. Application à une parcelle de vigne en Cévennes-Vivarais, PhD thesis, Université Joseph Fourier, France, 217 pp., 2010.

Nicoud, C.: Study of the relationship between initial soil moisture and hydraulic response for evaluation of flood severity, MS thesis, Université Joseph Fourier, France, 44 pp., 2015.

Nord, G., Gallart, F., Gratiot, N., Soler, M., Reid, I., Vachtman, D., Latron, J., Martín Vide, J. P., and Laronne, J. B.: Applicability of acoustic Doppler devices for flow velocity measurements and discharge estimation in flows with sediment transport, J. Hydrol., 509, 504–518, doi:10.1016/j.jhydrol.2013.11.020, 2014.

Raupach, T. H. and Berne, A.: Correction of raindrop size distributions measured by Parsivel disdrometers, using a two-dimensional video disdrometer as a reference, Atmos. Meas. Tech., 8, 343–365, doi:10.5194/amt-8-343-2015, 2015.

Reba, M. L., Marks, D., Seyfried, M., Winstral, A., Kumar, M., and Flerchinger, G.: A long-term data set for hydrologic modeling in a snow-dominated mountain catchment, Water Resour. Res., 47, W07702, doi:10.1029/2010WR010030, 2011.

Reed, S., Koren, V., Smith, M., Zhang, Z., Moreda, F., Seo, D. J., and DMIP Participants: Overall distributed model intercomparison project results, J. Hydrol., 298, 27–60, doi:10.1016/j.jhydrol.2004.03.031, 2004.

Renard, K. G., Nichols, M. H., Woolhiser, D. A., and Osborn, H. B.: A brief background on the U.S. Department of Agriculture Agricultural Research Service Walnut Gulch Experimental Watershed, Water Resour. Res., 44, W05S02, doi:10.1029/2006WR005691, 2008.

Ruin, I., Creutin, J., Anquetin, S., and Lutoff, C.: Human exposure to flash-floods-relation between flood parameters and human vulnerability during a storm of September 2002 in Southern France, J. Hydrol., 361, 199–213, 2008.

Schneebeli, M., Dawes, N., Lehning, M., and Berne, A.: High-resolution vertical profiles of polarimetric X-band weather radar observables during snowfall in the Swiss Alps, J. Appl. Meteorol. Clim., 52, 378–394, doi:10.1175/JAMC-D-12-015.1, 2013

Schneebeli, M., Grazioli, J., and Berne, A.: Improved Estimation of the Specific Differential Phase Shift Using a Compilation of Kalman Filter Ensembles, IEEE T. Geosci. Remote, 52, 5137–5149, doi:10.1109/TGRS.2013.2287017, 2014.

Slaughter, C. W., Marks, D., Flerchinger, G. N., Van Vactor, S. S., and Burgess, M.: Thirty-five years of research data collection at the Reynolds Creek Experimental Watershed, Idaho, United States, Water Resour. Res., 37, 2819–2823, doi:10.1029/2001WR000413, 2001.

Stone, J. J., Nichols, M. H., Goodrich, D. C., and Buono, J.: Long-term runoff database, Walnut Gulch Experimental Watershed, Arizona, United States, Water Resour. Res., 44, W05S05, doi:10.1029/2006WR005733, 2008.

Tabary, P.: The new French radar rainfall product. Part I: Methodology, Weather Forecast., 22, 393–408, 2007.

Tuset, J., Vericat, D., and Batalla, R. J.: Rainfall, runoff and sediment transport in a Mediterranean mountainous catchment, Sci. Total Environ., 540, 114–132, doi:10.1016/j.scitotenv.2015.07.075, 2016.

Uber, M..: The Impact of Initial Soil Moisture on the Hydrologic Response of Two Flash Flood Prone Catchments in Southern France, MS thesis, University of Potsdam, Germany, 80 pp., 2016.

Weiler, M. and Beven, K.: Do we need a Community Hydrological Model?, Water Resour. Res., 51, 7777–7784, doi:10.1002/2014WR016731, 2015.

Welber, M., Le Coz, J., Laronne, J. B., Zolezzi, G., Zamler, D., Dramais, G., Hauet, A., and Salvaro, M.: Field assessment of noncontact stream gauging using portable surface velocity radars (SVR), Water Resour. Res., 52, 1108–1126, doi:10.1002/2015WR017906, 2016.

Western, A. W. and Grayson, R. B.: The Tarrawarra Data Set: Soil moisture patterns, soil characteristics, and hydrologi-

cal flux measurements, Water Resour. Res., 34, 2765–2768, doi:10.1029/98WR01833, 1998.

Zwiebel, J., Van Baelen, J., Anquetin, S., Pointin, Y., and Boudevillain, B.: Impacts of orography and rain intensity on rainfall structure. The case of the HyMeX IOP7a event, Q. J. Roy. Meteor. Soc., 142, 310–319, doi:10.1002/qj.2679, 2015.